Scientia Pharmaceutica

ÖSTERREICHISCHE PHARMAZEUTISCHE GESELLSCHAFT

MDPI

Article

Ethanol–Withanolide Interactions: Compound-Specific Effects on Photokinetic Behavior and NMDA Receptor Subunit Expression in Zebrafish Larvae

Kamila Czora-Poczwardowska [1], Radosław Kujawski [1,*], Weronika Jarczak [1], Emilia Cicha [2], Maria Miotk [3], Przemysław Mikołajczak [1] and Michał Szulc [1]

[1] Department of Pharmacology, Poznan University of Medical Sciences, 60-806 Poznan, Poland; kczora@ump.edu.pl (K.C.-P.); weronika.jarczak@ump.edu.pl (W.J.); przemmik@ump.edu.pl (P.M.); mszulc@ump.edu.pl (M.S.)

[2] Animal Facility, Poznan University of Medical Sciences, 60-806 Poznan, Poland; emiliacicha@ump.edu.pl

[3] Student Scientific Society, Student Research Group of Pharmacology, Poznan University of Medical Sciences, 60-806 Poznan, Poland; marysiamiotk1@gmail.com

* Correspondence: radkuj@ump.edu.pl

Abstract

Concurrent use of *Withania somnifera* (WS, ashwagandha) preparations and ethanol (EtOH) is increasingly common, yet the consequences for glutamatergic signaling remain uncharacterized. Because N-methyl-D-aspartate (NMDA) receptors are a principal target of acute EtOH, we examined whether three purified withanolides modify this response. Zebrafish (*Danio rerio*) were exposed to withanolide A (WITA), withanone (WIN) or withaferin A (WTFA) at 3–5 days post-fertilization (dpf) and to EtOH (0–4.0% *v*/*v*) for 1 h at 5 dpf. Photokinetic behavior was quantified with a normalized dark–light contrast index (DLCI; withanolides at 0–500 µg/L) and *grin2aa*, *grin2bb*, *grin3a* and *grin3ba* transcripts were measured by RT-qPCR (withanolides at 100 µg/L). EtOH caused a concentration-dependent reduction in DLCI, and photokinetic differentiation was markedly impaired at 2.0% and 4.0%. EtOH increased *grin2aa* and *grin2bb* expression and decreased *grin3a* and *grin3ba* expression, with *grin2bb* responding at lower concentrations than *grin2aa*. The three withanolides produced distinct modulatory profiles. WITA partially preserved photokinetic differentiation at high EtOH concentration and attenuated selected transcriptional responses, whereas WIN showed limited effects. WTFA produced the strongest EtOH-dependent changes in NMDA receptor subunit expression but did not prevent behavioral impairment. These findings indicate compound-specific modulation of acute EtOH-induced behavioral responses and NMDA receptor subunit transcription.

Keywords: *Danio rerio*; ethanol; withanolides; withaferin A; NMDA receptor; gene expression; *Withania somnifera*; herb–drug interaction

Check for updates

Academic Editor: Walter Jäger

Received: 22 September 2026
Revised: 29 October 2026
Accepted: 3 November 2026
Published: 5 November 2026

Copyright: © 2026 by the authors. Published by MDPI on behalf of the Österreichische Pharmazeutische Gesellschaft. Licensee MDPI, Basel, Switzerland. This article is an open access article distributed under the terms and conditions of the Creative Commons Attribution (CC BY) license.

1. Introduction

Ethanol (EtOH) is one of the most widely consumed psychoactive substances worldwide [1,2]. Harmful use caused approximately 2.6 million deaths in 2019, about 4.7% of all deaths [1]. Its dose-dependent effects on the central nervous system (CNS) follow a well-characterized biphasic action: stimulation, euphoria, and disinhibition at low-to-moderate blood concentrations, followed by sedation, motor incoordination, and, at sufficiently high doses, respiratory depression [3,4]. Although EtOH acts on a wide range of central receptor systems, including dopaminergic and serotonergic ones, its biphasic effect is most

likely mediated by two principal ionotropic receptor systems: allosteric potentiation of γ-aminobutyric acid type A (GABAA) receptors, enhancing inhibitory neurotransmission, and inhibition of N-methyl-D-aspartate (NMDA) glutamate receptors, which attenuates the dominant excitatory drive in the CNS [4–7].

Withania somnifera (L.) Dunal (WS, ashwagandha), a perennial plant of the nightshade family (*Solanaceae*) used for centuries in Ayurvedic medicine [8,9], is among the most widely used herbal supplements globally, with a global market estimated at USD 777.8 million in 2025 and a projected annual growth rate of 8.94% from 2026 to 2033 [10]. Its rising popularity comes from reported adaptogenic, anxiolytic, and neuroprotective effects [8,11]. Concurrent use of herbal preparations and EtOH is increasingly documented [12,13], raising concerns about potential interactions that remain poorly characterized at the mechanistic level. The principal bioactive constituents of WS are withanolides, a class of steroidal lactones comprising over 40 identified compounds [9]. While withaferin A (WTFA) has received the most pharmacological attention, the mechanisms of action of other purified withanolides—including withanolide A (WITA) and withanone (WIN)—remain poorly characterized. The three withanolides examined here are structural isomers sharing the molecular formula $C_{28}H_{38}O_6$ and differing mainly in the position of the epoxide ring and hydroxyl substituents (Figure 1) [9]; they also differ in their distribution within the plant—WTFA is abundant in the leaves, whereas WITA is regarded as a characteristic constituent of the roots, the part most commonly used in commercial preparations [8,9]. Crucially, WS constituents exert modulatory effects at both GABAA and NMDA receptors [9,14]—the same principal targets through which EtOH exerts its biphasic CNS effects. Despite the potential co-use of WS-based preparations and EtOH in non-dependent populations, safety data and mechanistic characterization of such interactions remain absent from the literature. Having previously characterized the GABAergic component of the acute EtOH–withanolide interaction in zebrafish larvae [15], we have focused here on the NMDA receptor system, the second principal target of acute EtOH.

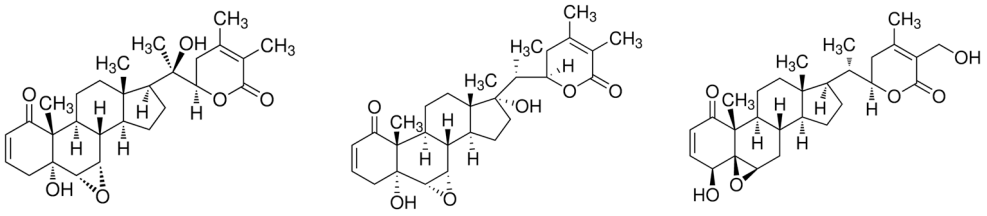


Figure 1. Chemical structures of the analyzed compounds: withanolide A, withanone, withaferin A.

Glutamate is the major excitatory neurotransmitter in vertebrates, with NMDA receptors mediating the calcium-permeable component of synaptic transmission, which is essential for synaptic plasticity, long-term potentiation, learning, and memory consolidation [16–18]. These receptors are heterotetramers: activating them requires both glutamate and a co-agonist (either glycine or D-serine) and they are put together from two GluN1 units (from *grin1* gene) and two regulatory subunits from either the GluN2 family (GluN2A-GluN2D, encoded by *grin2a-d* genes, respectively) or the GluN3 family (GluN3A-B, encoded by *grin3a-b* genes, respectively) [16–18]. Subunit composition determines receptor biophysics, pharmacology, subcellular localization, and downstream signaling specificity. For instance, GluN2A subunit-containing receptors predominate at mature synapses and exhibit fast deactivation kinetics, high Mg^{2+} sensitivity at resting potentials, and moderate single-channel conductance [18,19]. GluN2B subunit-containing receptors are characterized by slower deactivation kinetics and greater Ca^{2+} permeability, which is crucial for synapto-

genesis and developmental plasticity. In the mature nervous system, their expression is predominantly limited to the forebrain and extrasynaptic locations [18,19]. Channel opening in GluN1/GluN2 assemblies requires simultaneous agonist binding and postsynaptic membrane depolarization sufficient to relieve Mg^{2+} block from the pore—a coincidence-detection mechanism that couples NMDA receptor activation to the membrane potential state of the postsynaptic neuron [16,17]. The GluN3 subfamily exerts a qualitatively distinct modulatory function: co-assembly of GluN3A with GluN1 and GluN2 subunits markedly reduces single-channel conductance, Ca^{2+} permeability, and Mg^{2+} sensitivity relative to GluN1/GluN2 assemblies [16,20,21]. GluN3A therefore acts as a developmental "brake" on synapse maturation [20]: it is expressed at high levels early in development, delaying synapse stabilization until sensory input arrives, and is subsequently downregulated, allowing GluN2A and GluN2B to predominate and support mature forms of plasticity [22].

In larval zebrafish (*Danio rerio*), NMDA receptor transmission becomes active early. By 5 days post-fertilization (dpf)—the time point used in this study—larvae already display habituation, avoidance learning, and light–dark locomotor transitions [23–25]. Notably, larval locomotion becomes sensitive to NMDA-receptor antagonism from approximately 5 dpf [26], indicating functional engagement of glutamatergic signaling at this developmental stage. At this point, the system is switching from GluN2B to GluN2A dominance, although the transition is not yet complete [18,27]. Concurrently, chloride homeostasis is still maturing: *kcc2* expression in zebrafish first appears at approximately 2 dpf and increases progressively thereafter [28], and the GABAergic excitation-to-inhibition switch—documented at approximately 2.5 dpf in retinal neurons [29]—proceeds region-specifically and may not be complete across all CNS circuits at the 5 dpf time point employed here [30,31]. Any residual depolarizing GABAergic drive would facilitate NMDA receptor activation by contributing to Mg^{2+} block relief at lower levels of excitatory input than required in a mature system [16,32].

Due to the teleost-specific whole-genome duplication, the zebrafish NMDA receptor gene family comprises 13 subunit-encoding genes, compared to 7 in non-duplicated vertebrate genomes [33,34]. The subunits whose expression profiles were evaluated in an experiment on *Danio rerio* larvae <5 dpf, described later in this manuscript, reflect those paralogies: *grin2aa* and *grin2bb* are co-orthologues of mammalian Grin2A and Grin2B, *grin3a* is the only zebrafish equivalent of mammalian Grin3A, and *grin3ba* is one of two for Grin3B [33,35]. The extent to which these paralogues have diverged in expression patterns and pharmacological sensitivity relative to their mammalian counterparts is not fully established [35,36].

NMDA receptors are among the principal molecular targets that mediate the concentration-dependent CNS effects of EtOH. Acute EtOH, at concentrations as low as 20–25 mM (0.12–0.15% EtOH (*v*/*v*), the concentration range observed during moderate human intoxication), non-competitively inhibits NMDA receptor function, as shown first in hippocampal neurons [37] and later in other systems [5,6,38]. This inhibitory action is voltage-independent and does not involve competition at the glutamate or glycine binding sites, distinguishing it mechanistically from classical open-channel blockers [37]. The sensitivity of NMDA receptors to acute EtOH inhibition depends critically on which GluN2 subunit is incorporated into the receptor complex [5,6,38]. In rat GluN1/GluN2A and GluN1/GluN2B receptors (when expressed in HEK-293 cells), EtOH reduces receptor function mainly by shortening channel open time through altered gating conformations, with a stronger effect on GluN2B-containing receptors [39]. In GluN2A-containing receptors, the inhibitory mechanism additionally involves prolongation of closed-state dwell times, indicating a partially distinct gating mode of action [5,39]. Site-directed mutagenesis supports this interpretation: substitution of individual residues in GluN2B (F637, G826) shifts EtOH sensitivity, despite

the high overall sequence similarity between GluN2A and GluN2B [40]. At concentrations corresponding to the legal driving limits in the US and the UK (approximately 17–20 mM), however, overall NMDA receptor inhibition is modest (less than 10%) and fundamental properties such as glutamate or magnesium sensitivity remain unchanged [41], indicating that mechanistic differences between subtypes become functionally consequential primarily at higher, intoxicating EtOH concentrations. Incorporation of the GluN3A subunit changes how NMDA receptors respond to EtOH. In GluN1/GluN2A assemblies, magnesium makes EtOH's inhibitory effect more pronounced, but once GluN3A is included, that enhancement vanishes (and this is unique to GluN2A, with no similar effect observed in GluN2B combinations) [42]. Importantly, GluN3A does not change the basic sensitivity of NMDA receptors to EtOH when magnesium is not present [43]. In addition, receptors that contain GluN3 subunits are less sensitive to channel blockers such as memantine [44].

Although the present study examined acute rather than chronic EtOH exposure, the broader literature on prolonged EtOH use provides important translational context. Chronic EtOH induces upregulation of *Grin2b* and *Grin2a* mRNA in cortical and hippocampal regions in rodents [45,46], with *Grin2b* upregulation representing the most consistent finding across experimental models—an adaptation mechanistically linked to tolerance, withdrawal hyperexcitability, and excitotoxic vulnerability during abstinence [4]. Human post-mortem findings support this: people with a history of alcoholism have higher mRNA for GluN1, GluN2A, and GluN3A in the hippocampal dentate gyrus, with GluN3A also up in the orbitofrontal cortex—direct evidence that subunit remodeling in NMDA receptors is clinically meaningful and identifying GluN3A as a transcriptional target of prolonged EtOH exposure [47].

The aim of this study was to characterize, in larvae from the same experiment and exposure framework used for our GABAergic analysis [15], the transcriptional response of four NMDA-receptor subunit genes (*grin2aa*, *grin2bb*, *grin3a*, *grin3ba*) to an acute ethanol gradient (0–4.0%) and its modulation by three purified withanolides (WITA, WIN, WTFA), alongside a photokinetic behavioral readout (the dark–light contrast index, DLCI). We hypothesized that (i) acute ethanol upregulates pro-excitatory *grin2* co-orthologues (*grin2aa*, *grin2bb*) as a compensatory response to receptor inhibition; (ii) acute ethanol downregulates modulatory *grin3* subunits (*grin3a*, *grin3ba*); (iii) purified withanolides exert distinct, compound-specific modulatory effects on both baseline and ethanol-altered NMDA subunit profiles; and (iv) the loss of photokinetic differentiation co-occurs, at the group level, with the greatest extent of NMDA subunit transcriptional remodeling.

2. Materials and Methods

2.1. Reagents

Invitrogen TRIzol reagent was purchased from Thermo Fisher Scientific (Waltham, MA, USA). WITA (Withanolide A phyproof® Reference Substance) and WIN (Withanone phyproof® Reference Substance) were obtained from PhytoLab (Vestenbergsgreuth, Germany), while WTFA was obtained from Sigma-Aldrich (St. Louis, MO, USA). WITA, WIN, and WTFA were prepared as 1 mg/mL stock solutions in dimethyl sulfoxide (DMSO) and diluted in the exposure medium (E3 medium: 5 mM NaCl, 0.17 mM KCl, 0.33 mM $CaCl_2 \cdot 2H_2O$, 0.33 mM $MgSO_4$; pH 6.5–8.5) to final concentrations of 10,100, and 500 µg/L. The final DMSO concentration in the medium did not exceed 0.05% (v/v) at the highest withanolide concentration (0.01% at the 100 µg/L concentration used for transcriptional analysis), a level considered safe for *Danio rerio* larvae and therefore regarded as negligible in terms of any potential DMSO-related effects. For the isolation of mRNA from biological material, we used chloroform (≥99.5%), EtOH (96%), and isopropanol (≥99.5%) purchased from Sigma-Aldrich (St. Louis, MO, USA). DEPC-treated water was supplied by

Thermo Fisher Scientific (Waltham, MA, USA). To reverse-transcribe mRNA into cDNA, we used The Reliance Select cDNA Synthesis Kit (Bio-Rad Laboratories, Hercules, CA, USA), and for qPCR, we used GoTaq® qPCR Master Mix from Promega (Madison, WI, USA). Gene-specific primers (sense and antisense) for the selected genes were synthesized by the Sequencing Core Facility of the Institute of Biochemistry and Biophysics, Polish Academy of Sciences (Warsaw, Poland).

2.2. Experimental Design

Zebrafish larvae at 3–5 dpf obtained from multiple breeding pairs of the AB strain were maintained under standard laboratory conditions (temperature 28.5 °C, well aerated aquarium water, 14 h light: 10 h dark photoperiod), according to established protocols and literature recommendations [48,49]. The experiments were conducted in the Animal Facility, Poznan University of Medical Sciences. Larvae were exposed to one of the three purified withanolides (WITA, WIN or WTFA) at 0, 10,100 or 500 µg/L for 48 h, from 3 to 5 dpf, as in our companion study [15]. Embryos were pooled before allocation and distributed randomly to the exposure groups, so that each treatment group comprised offspring of several pairs; larvae with morphological abnormalities or low viability were excluded before testing. At 5 dpf, one hour before behavioral testing, larvae were transferred individually to the wells of 96-well plates (one larva per well), and EtOH was added to the medium to obtain a concentration gradient of 0%, 0.5%, 1.0%, 2.0% or 4.0% (*v*/*v*), so that each withanolide concentration was combined with the full EtOH gradient; treatment combinations were distributed randomly across the plates. Each treatment combination was tested in at least four independent experimental runs (separate plates), each including a planned 10–12 larvae per group, corresponding to approximately 40–48 larvae per experimental condition [15]. In the behavioral analysis, each larva was treated as an independent experimental unit. All final DMSO concentrations remained well below the 0.55% threshold reported to affect larval zebrafish behavior in a light/dark paradigm and were also far below levels associated with developmental or toxic effects in *Danio rerio*, making any potential impact of DMSO negligible [50–52]. For this reason, withanolide-free groups (labeled H_2O) were maintained in E3 medium alone, and the vehicle was not tested as a separate group. Moreover, because all three withanolides were applied at identical final DMSO concentrations, a vehicle-related effect is unlikely to account for the compound-specific differences reported here.

Following exposure, larvae underwent a 10 min dark acclimation period and a light–dark transition locomotor assay consisting of two alternating 10 min light and 10 min dark cycles, as described in detail previously [15]. Locomotor activity was recorded with the DanioVision system and analyzed with EthoVision XT 14 software (Noldus, Wageningen, The Netherlands). Larvae were collected immediately after the behavioral protocol for RNA isolation. Transcriptional analysis was subsequently restricted to the 100 µg/L condition for each investigated phytochemical.

2.3. Behavioral Data Analysis

A dark–light contrast index (DLCI) was calculated for each larva as

$$DLCI = \frac{D - L}{D + L} \quad (1)$$

which yields the range

$$-1 \leq DLCI \leq 1 \quad (2)$$

adapting the lighting motor index proposed by Li et al. [53]. D and L are the total distances moved during the dark and light phases. The index expresses the difference between the

two phases as a fraction of their sum. It also stays largely independent of how much a given larva moves overall. This places it within the family of normalized discrimination indices used in behavioral neuroscience. The discrimination ratio of Ennaceur and Delacour [54] is a classic example. In a pooled analysis of object-recognition data, Akkerman et al. [55] showed that relative (normalized) discrimination measures, unlike absolute ones, are not correlated with the level of exploratory activity in the test trial, and are therefore more resistant to activity-related bias.

A value close to 1 means that a larva moves mostly in the dark and suppresses activity in the light. Such a larva still discriminates between the two phases. This is consistent with an intact photokinetic response. A value close to 0 means that locomotion no longer tracks the lighting condition. This is the pattern expected when the photokinetic response is blunted. The larva then swims at a similar level regardless of the stimulus. The DLCI therefore reports whether the behavioral response to light is preserved, independently of baseline locomotion. This distinction matters here because EtOH and the withanolides are each expected to alter overall activity on their own.

The DLCI refines the dark/light (D/L) ratio, also called the lighting motor index, previously applied to zebrafish locomotion by Li et al. [53]. Li et al. interpreted that index mainly as a marker of anxiety-related reactivity to the light–dark transition. We instead read it as a measure of photokinetic differentiation between phases. The normalized formulation is also more stable numerically. A simple D/L ratio diverges as the light-phase distance approaches zero. The DLCI stays bound under the same conditions. The locomotor recordings analyzed here were obtained from the same specimens used in our companion study [15]. The DLCI was not reported in that particular study. It is introduced here as a new derived parameter proposed by the authors.

2.4. Molecular Analyses

RNA isolation: Immediately after completion of the behavioral protocol, larvae from the same treatment group were transferred in groups of eight (pooled as one sample) into RNase-free 1.5 mL microtubes and immersed in 300 µL TRIzol. Total RNA was isolated from the collected tissue (whole body) of zebrafish larvae using a modified Chomczynski and Sacchi method [56]. Samples were homogenized [49,57] using an Omni Bead Ruptor 4 (Omni International, Kennesaw, GA, USA) at speed 5 for 90 s until a uniform suspension was achieved. Chloroform was then added, the samples were mixed and, after centrifugation (12,000× *g*, 4 °C, 15 min), the upper aqueous phase was transferred to fresh tubes. An equal volume of isopropanol was added, and samples were incubated at −80 °C for 1 h to precipitate nucleic acids. After thawing, samples were centrifuged (12,000× *g*, following 7500× *g*, each at 4 °C, 10 min). The RNA pellet was washed twice with 70% EtOH. After drying, the pellet was dissolved in 30 µL of DEPC-treated water. RNA concentration and purity were assessed spectrophotometrically.

cDNA synthesis: First-strand cDNA was synthesized from the isolated RNA by reverse transcription (RT) using a commercial kit following the manufacturer's instructions (Bio-Rad Laboratories, Hercules, CA, USA). RT reactions were performed in a TC 1000-G DLAB thermocycler (Dragonlab, Beijing, China) and adjusted to a final reaction volume of 20 µL with nuclease-free water.

Gene expression analysis by RT-qPCR: Gene expression profiling was conducted using real-time quantitative PCR technique with reverse transcription (RT-qPCR) [58,59]. Target gene-specific primers (Table 1) were designed using Primer3 version 4.1.0 and Primer-BLAST (NCBI, accessed on 20 April 2024; https://www.ncbi.nlm.nih.gov/tools/primer-blast/). Primer specificity was verified using Nucleotide BLAST (NCBI, accessed on 20 April 2024; https://blast.ncbi.nlm.nih.gov/Blast.cgi). Reactions were performed using

GoTaq® qPCR Master Mix (Promega, Madison, WI, USA) and a LightCycler 480 system (Roche Diagnostics, Basel, Switzerland) with fluorescence detection. The analyzed genes included subunits of NMDA receptors (*grin2aa*, *grin2bb*, *grin3a*, *grin3ba*). The eukaryotic elongation factor 1-alpha (*ef1a*) was used as a reference gene, previously validated as stable in zebrafish larvae [60]. Each reaction was run in technical triplicate. Each experimental group comprised at least 7 biological replicates, each consisting of RNA pooled from 8 larvae. The pooled sample was therefore the experimental unit of the molecular analysis; because larvae were pooled, transcript levels could not be linked to the behavioral scores of individual larvae.

Table 1. Primer sequences and accession numbers for reference and target genes used in RT-qPCR.

Gene	Accession Number	Forward Primer [5′→3′]	Reverse Primer [5′→3′]
ef1a	FJ915061.1	CTGGAGGCCAGCTCAAACAT	ATCAAGAAGAGTAGTACCGCTAGCATTAC
grin2aa	XM_021473854.1	TCTTCTCCATCAGCAGGGGTA	CCGCCACGTTTAGGAGAGTT
grin2bb	XM_017355008.2	CCAACGAGGTGCTGAGGTAT	CGTCCGAGTACAGCTCGAAG
grin3a	XM_009305086.3	TCCAACGACAGACTCAGAACT	GGACGGTTCCCAGGTGAAAT
grin3ba	XM_021467383.1	CGTCACCAGCAGAGGTTCAA	CAGGCACAAGGTGGGACATC

Thermal cycling conditions were optimized for each primer set and included an initial denaturation step at 95 °C for 2 min, followed by 45 cycles of amplification. Melting curve analysis was performed at the end of the run to confirm amplification specificity. The details for each primer set are provided in Table 2.

Table 2. Thermal cycling conditions for the RT-qPCR amplification.

Primer	Initial Denaturation	Denaturation (45 Cycles)	Annealing/Extension	Melting Curve Analysis
ef1a	95 °C, 120 s	95 °C, 15 s	59 °C, 60 s	95 °C to 60 °C
grin2aa, *grin2bb*, *grin3a*, *grin3ba*			60 °C, 60 s	

2.5. Statistical Analysis

Statistical analysis of behavioral and molecular (RT-qPCR) data was performed using Statistica 13 software (StatSoft, Tulsa, OK, USA). Results from biological and technical replicates within each group were averaged and are presented as the mean ± SEM (standard error of the mean). The experimental unit was the individual larva for behavioral data (DLCI) and the pooled sample of eight larvae for RT-qPCR data; technical replicates were averaged before analysis and were not treated as independent observations. The data distribution was assessed using the Shapiro–Wilk test and found to be normal. For comparisons involving EtOH concentration alone, a one-way ANOVA was performed. For analyses evaluating the effects of EtOH concentration and withanolide treatment, a two-way ANOVA was used, including the interaction between these factors. Post hoc differences between groups were evaluated using the Tukey test with the same significance threshold ($p \leq 0.05$).

Relative gene expression strategy was applied, and their mRNA profiles were calculated using the $2^{-\Delta\Delta Ct}$ method [58,59]. Average Ct values from technical replicates were normalized to the reference gene (ef1α) and expressed relative to the control group (0% EtOH) [58,59]. A single reference gene was used, in line with its validation as a stable reference gene in zebrafish [60], and its mRNA levels were statistically stable among the groups in our experimental model.

3. Results

3.1. DLCI Results

The first step was to assess the effect of EtOH on DLCI in *D. rerio* larvae (see Figure 2). A one-way ANOVA revealed a significant effect of EtOH concentration ($F(4346) = 216.80$, $p < 0.001$). Subsequent post hoc analysis showed a statistically significant decrease in DLCI in the EtOH 2% and EtOH 4% groups (both $p < 0.001$). DLCI values for the EtOH 0.5% and EtOH 1.0% groups were practically identical to those of the H_2O control group (Figure 2).

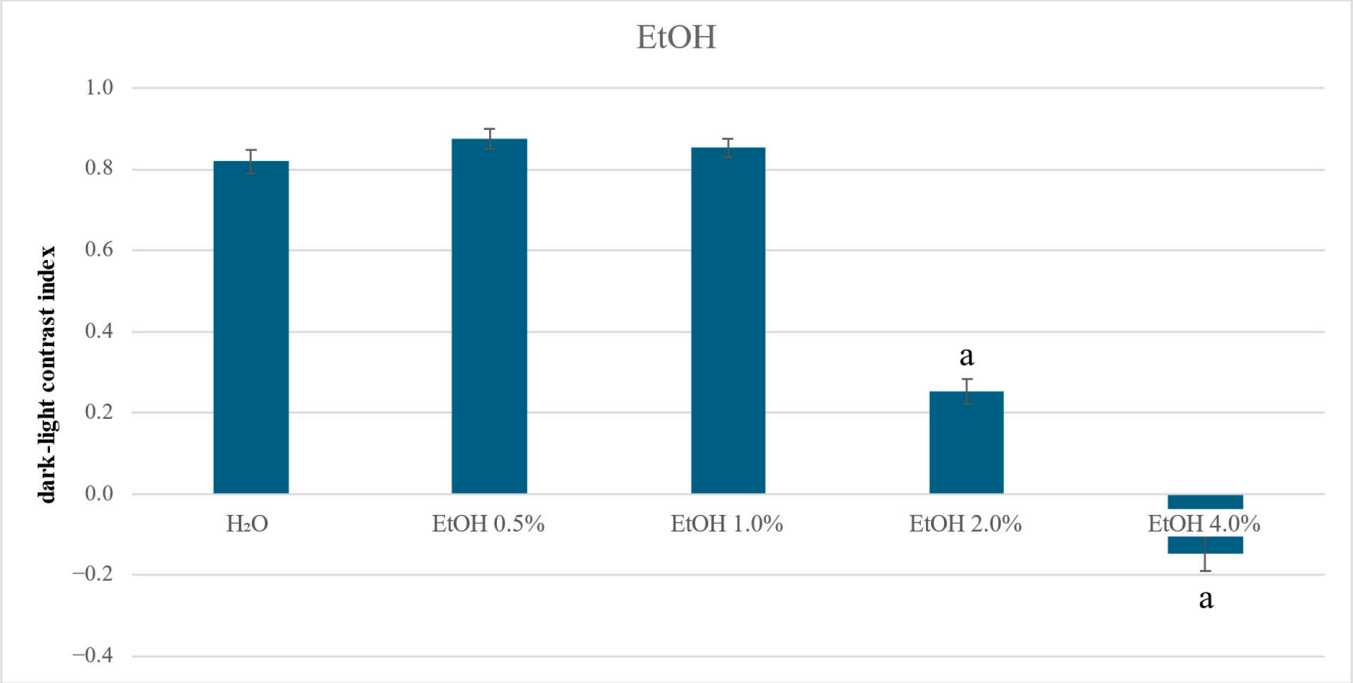


Figure 2. Effect of EtOH on the dark–light contrast index in D. rerio larvae. a—$p < 0.001$ vs. H_2O. Data are presented as mean ± SEM.

The next step was to assess the interaction between WIN and EtOH with respect to the DLCI parameter in *D. rerio* larvae as shown in Figure 3. A two-way ANOVA revealed significant overall effects [EtOH effect: $F(4800) = 236.52$, $p < 0.001$; WIN effect: $F(3800) = 12.91$, $p < 0.001$; interaction: $F(12,800) = 7.94$, $p < 0.001$]. Post hoc analysis showed a significant decrease in DLCI at every WIN concentration under 2.0% and 4.0% EtOH (all $p < 0.001$) relative to the corresponding H_2O control groups. WIN0 variability was consistent with that described for Figure 2. When DLCI values were compared between analogous EtOH exposed groups receiving WIN and their withanolide-free controls, a statistically significant decrease was observed for WIN500 4.0% versus WIN0 4.0% ($p < 0.001$). A decrease in DLCI was also observed for WIN500 4.0% versus WIN10 4.0% and WIN100 4.0% (all $p < 0.001$).

Next, the results of the interaction between WITA and EtOH were evaluated with respect to the DLCI parameter in *D. rerio* larvae (see Figure 4). A two-way ANOVA revealed significant overall effects [EtOH effect: $F(4833) = 103.29$, $p < 0.001$; WITA effect:

F (3833) = 10.02, $p < 0.001$; interaction: F (12,833) = 4.47, $p < 0.001$]. WITA0 group variability was consistent with that described for Figure 2. Post hoc analysis revealed a significant decrease in DLCI in the WITA10 group at 4.0% EtOH relative to the H_2O control of the same withanolide concentration ($p < 0.001$). Within the WITA100 groups, significant decreases were observed across the 1.0–4.0% EtOH range compared to the WITA100 H_2O control (all $p < 0.001$). Furthermore, DLCI in the WITA100 1% group was significantly lower than in the WITA0 1% group ($p < 0.001$). No statistically significant differences were found either within the WITA500 group or between this group and the remaining groups.

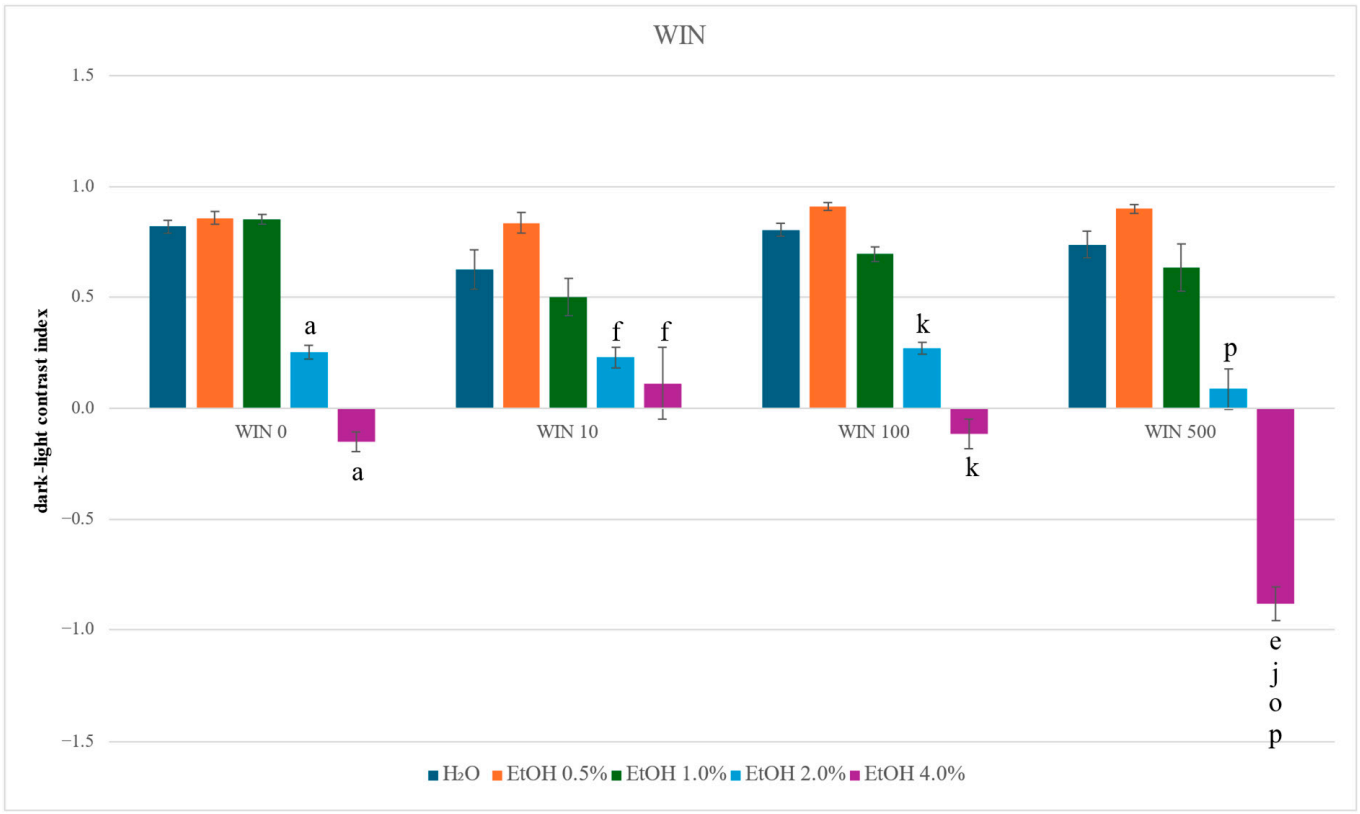


Figure 3. Effect of WIN on the dark–light contrast index in *D. rerio* larvae exposed to an EtOH gradient (0–4.0%). Significant comparisons ($p < 0.001$): a vs. WIN0 H_2O; e vs. WIN0 EtOH4%; f vs. WIN10 H_2O; j vs. WIN10 EtOH4%; k vs. WIN100 H_2O; o vs. WIN100 EtOH4%; p vs. WIN500 H_2O. Data are presented as mean ± SEM.

The final step regarding the behavioral results was the analysis of the interaction between WTFA and EtOH with respect to the DLCI parameter in *D. rerio* larvae as described in Figure 5. A two-way ANOVA revealed significant overall effects [EtOH effect: F (4692) = 201.19, $p < 0.001$; WTFA effect: F (3692) = 6.12, $p < 0.001$; interaction: F (12,692) = 5.55, $p < 0.001$]. WTFA0 group variability was consistent with that described for Figure 2. Post hoc analysis showed a decrease in DLCI at every WTFA concentration under 2.0% and 4.0% EtOH (all $p < 0.001$) relative to the corresponding H_2O control groups. Additionally, several significant effects were observed among the withanolide-free and low-EtOH conditions: DLCI in the WTFA10 H_2O group was significantly lower than in the WTFA0 H_2O control ($p < 0.001$), while DLCI in the WTFA100 H_2O group was significantly higher than in the WTFA10 H_2O group ($p < 0.001$). Elevated DLCI values were also observed in the WTFA10 0.5% and WTFA500 1% groups relative to their respective EtOH-matched controls ($p < 0.001$).

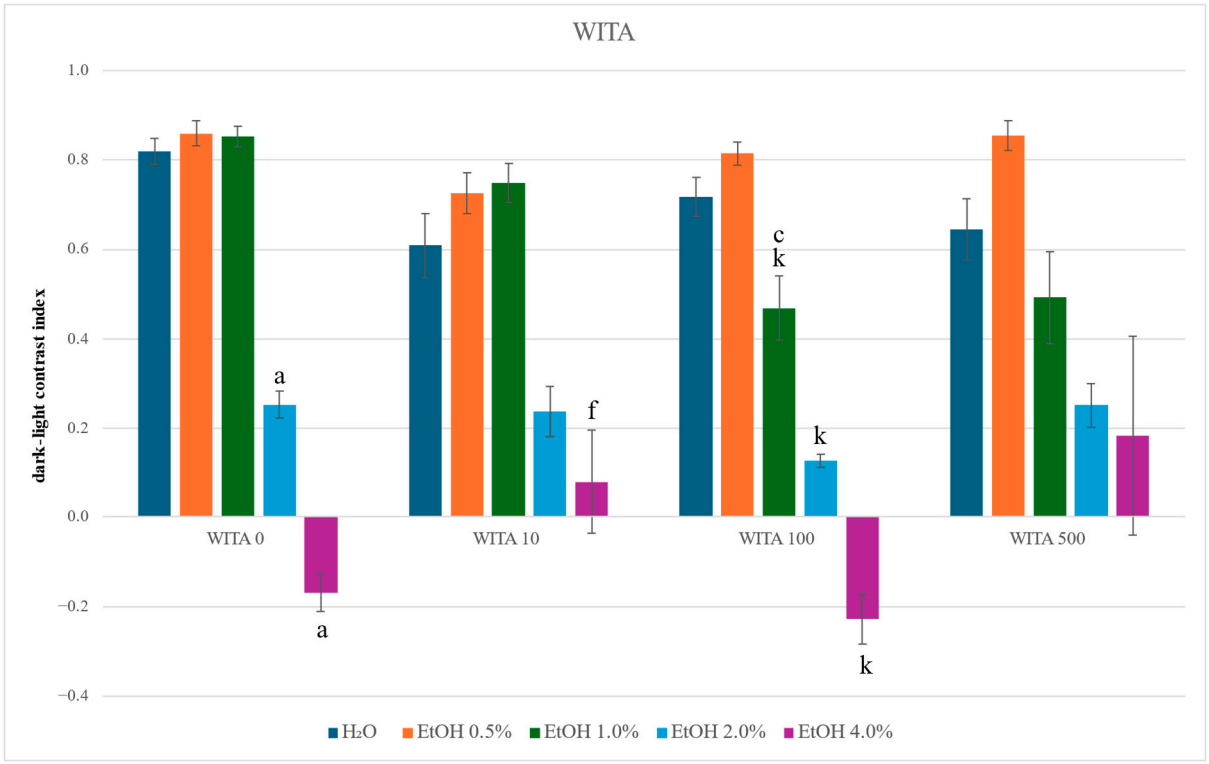


Figure 4. Effect of WITA on the dark–light contrast index in *D. rerio* larvae exposed to an EtOH gradient (0–4.0%). Significant comparisons ($p < 0.001$): a vs. WITA0 H_2O; c vs. WITA0 EtOH1%; f vs. WITA10 H_2O; k vs. WITA100 H_2O. Data are presented as mean ± SEM.

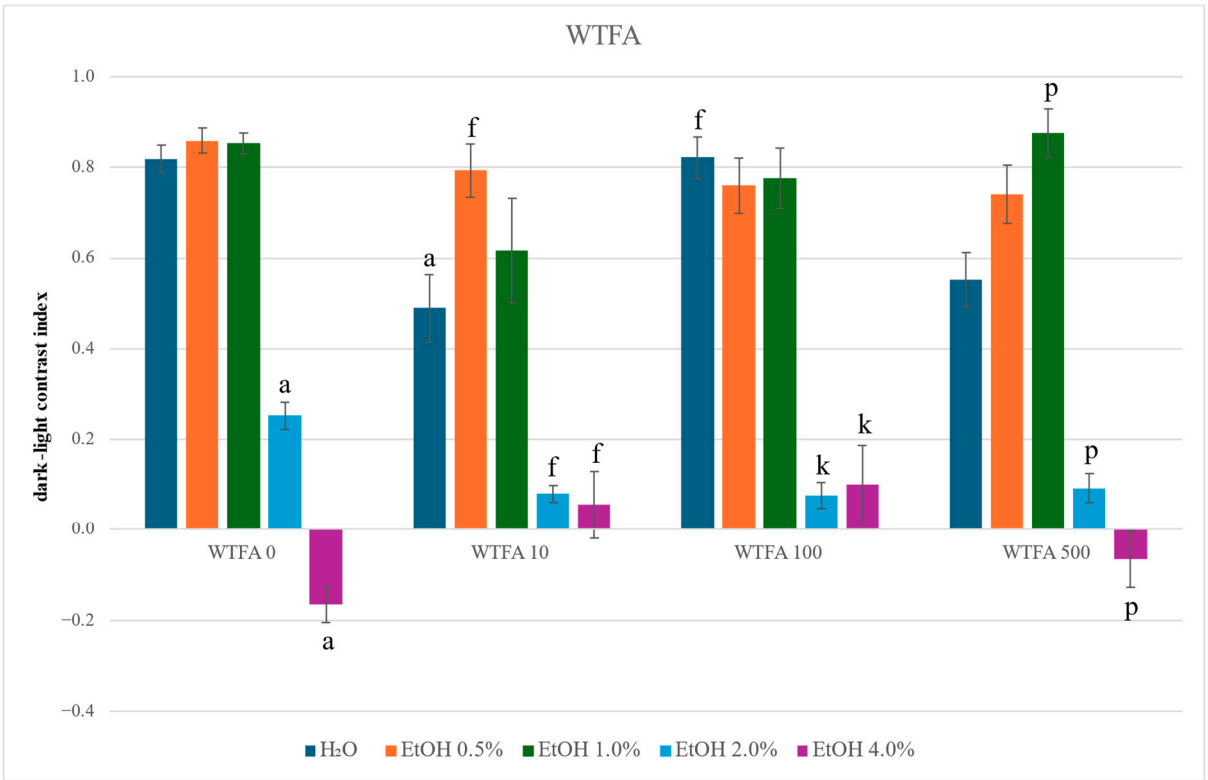


Figure 5. Effect of WTFA on the dark–light contrast index in *D. rerio* larvae exposed to an EtOH gradient (0–4.0%). Significant comparisons ($p < 0.001$): a vs. WTFA0 H_2O; f vs. WTFA10 H_2O; k vs. WTFA100 H_2O; p vs. WTFA500 H_2O. Data are presented as mean ± SEM.

3.2. Gene Expression Results

In the studies on the influence of EtOH gradient and withanolides on *grin2aa* gene mRNA expression in *D. rerio* larvae, significant overall effects were observed [EtOH effect: $F(4118) = 29.918$, $p < 0.001$; withanolide effect: $F(3118) = 477.31$, $p < 0.001$; interaction: $F(12,118) = 29.943$, $p < 0.001$]. The results are shown in Figure 6. Post hoc analyses showed that EtOH alone significantly ($p < 0.05$) increased *grin2aa* expression at 2.0% and 4.0% EtOH in control larvae (H_2O group), with the strongest upregulation observed at 4.0% EtOH. When comparing WITA-treated groups with the corresponding EtOH concentrations in larvae not receiving withanolides, a statistically significant increase in *grin2aa* expression was observed at WITA 0% EtOH and WITA 0.5% EtOH (both $p < 0.05$). No significant within-group differences were detected across EtOH concentrations within the WITA group. The lowest level of statistically significant variability was observed in larvae exposed to WIN, where a significant difference occurred only between the WIN 0% EtOH group and the corresponding WITA group ($p < 0.05$). The greatest variability was detected in the WTFA group, in which *grin2aa* expression was significantly increased relative to all corresponding EtOH concentrations in larvae exposed to H_2O alone, as well as relative to larvae receiving WITA + EtOH and WIN + EtOH (all $p < 0.05$).

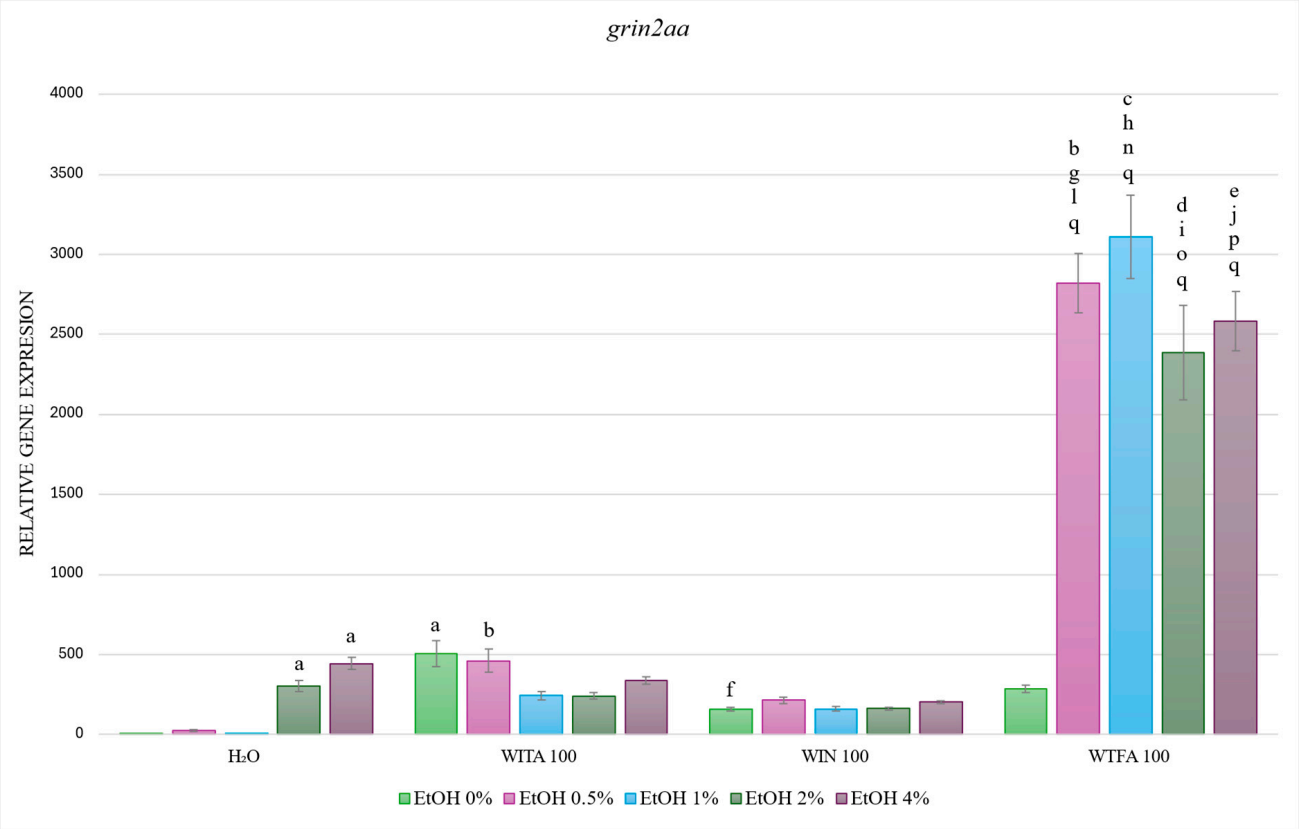


Figure 6. Effect of WITA, WIN and WTFA on *grin2aa* mRNA expression in *D. rerio* larvae under the influence of an EtOH concentration gradient (0–4.0%). a—$p < 0.05$ vs. H_2O; b—$p < 0.05$ vs. H_2O 0.5%; c—$p < 0.05$ vs. H_2O 1%; d—$p < 0.05$ vs. H_2O 2%; e—$p < 0.05$ vs. H_2O 4%; f—$p < 0.05$ vs. WITA 0%; g—$p < 0.05$ vs. WITA 0.5%; h—$p < 0.05$ vs. WITA 1%; i—$p < 0.05$ vs. WITA 2%; j—$p < 0.05$ vs. WITA 4%; l—$p < 0.05$ vs. WIN 0.5%; n—$p < 0.05$ vs. WIN 1%; o—$p < 0.05$ vs. WIN 2%; p—$p < 0.05$ vs. WIN 4%; q—$p < 0.05$ vs. WTFA 0%. Data are presented as mean ± SEM.

In the analysis of the influence of the EtOH gradient and withanolides on *grin2bb* gene mRNA expression in *D. rerio* larvae, statistically significant main effects and interactions were observed [EtOH effect: $F(4123) = 7.3510$, $p < 0.001$; withanolide effect: $F(3123) = 56.484$,

$p < 0.001$; interaction: F (12,123) = 17.248, $p < 0.001$]. Post hoc analyses showed that EtOH alone increased *grin2bb* gene expression at all tested concentrations in the control (H_2O) group ($p < 0.05$) (see Figure 7). It was also demonstrated that WITA administered without EtOH (Figure 7) increased *grin2bb* expression ($p < 0.05$). Within the WITA group, all EtOH concentrations resulted in significantly lower expression levels compared with WITA alone (0% EtOH) ($p < 0.05$). When comparing corresponding EtOH concentrations between the WITA and H_2O groups, the only statistically non-significant difference was observed at 2.0% EtOH. Within the WIN group, no significant within-group differences were detected across the EtOH gradient. When larvae receiving WIN at different EtOH concentrations were compared with larvae exposed to the corresponding EtOH concentrations without any withanolide, the only statistically significant difference was observed at 4.0% EtOH ($p < 0.05$). More pronounced differences were detected between the WITA and WIN groups, where statistically significant differences were found between the corresponding 0–1.0% EtOH groups ($p < 0.05$). As in the case of *grin2aa*, the greatest variability was observed in the WTFA group (Figure 7). Within this group, each EtOH concentration resulted in a significant increase in expression relative to the WTFA control (0% EtOH) ($p < 0.05$). When compared with the corresponding EtOH concentrations in the other groups, larvae exposed to 0.5% EtOH showed higher expression than those in the H_2O and WIN groups ($p < 0.05$); at 1.0–2.0% EtOH, expression was increased relative to H_2O, WITA, and WIN ($p < 0.05$); and at 4.0% EtOH, a significant difference was observed only in comparison with the corresponding EtOH concentration in WIN-treated larvae ($p < 0.05$).

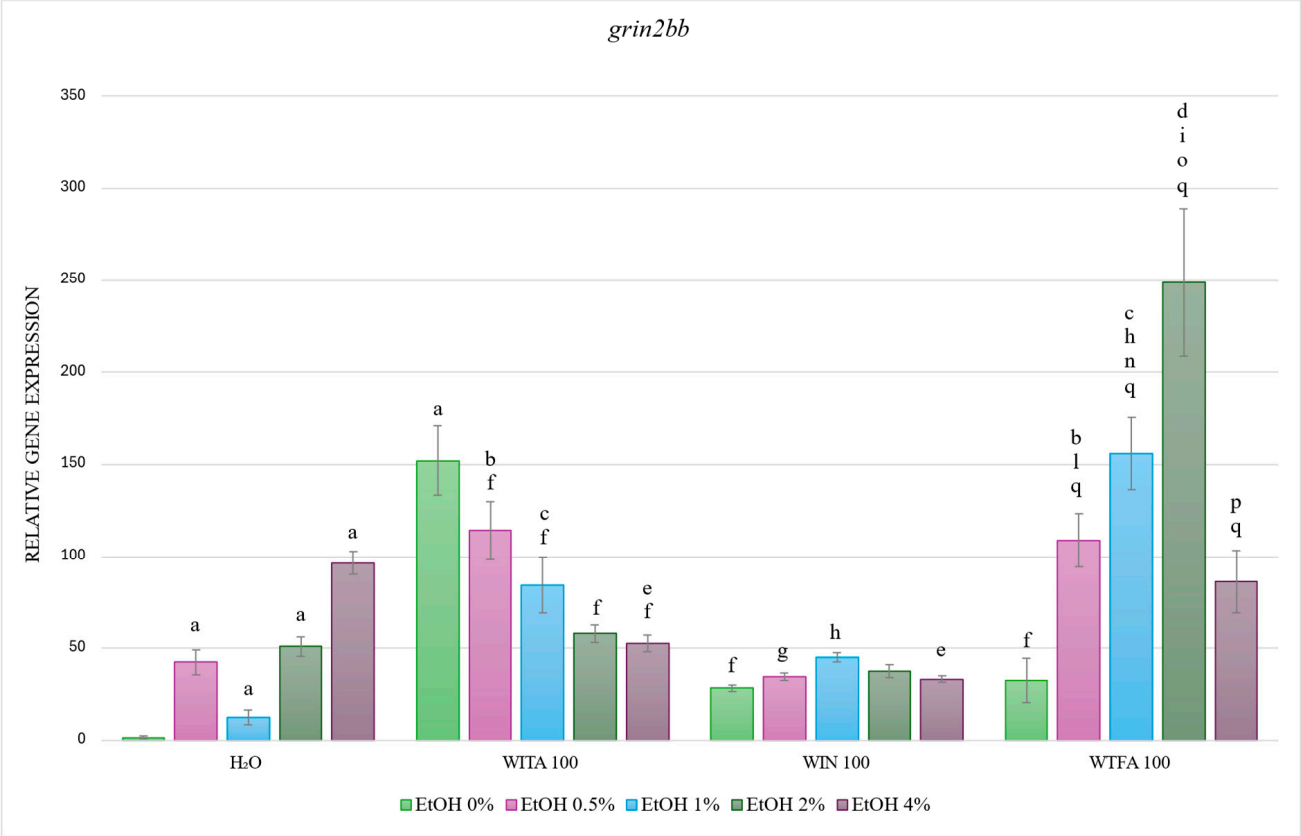


Figure 7. Effect of WITA, WIN and WTFA on *grin2bb* mRNA expression in D. rerio larvae exposed to an EtOH gradient (0–4.0%). Statistical significance ($p < 0.05$): a vs. H_2O; b vs. H_2O 0.5%; c vs. H_2O 1%; d vs. H_2O 2%; e vs. H_2O 4%; f vs. WITA 0%; g vs. WITA 0.5%; h vs. WITA 1%; i vs. WITA 2%; l vs. WIN 0.5%; n vs. WIN 1%; o vs. WIN 2%; p vs. WIN 4%; q vs. WTFA 0%. Data are presented as mean ± SEM.

In the studies investigating the effects of an EtOH gradient and withanolides on *grin3a* gene expression, the main effect of EtOH was not statistically significant [F (4133) = 0.962, $p = 0.431$], whereas the effect of the withanolides [F (3133) = 5.050, $p < 0.005$] and the EtOH × withanolide interaction [F (12,133) = 6.150, $p < 0.001$] were significant (see Figure 8). Although the main effect of EtOH did not reach significance, the significant interaction justified subsequent simple-effects analysis. Post hoc analysis revealed that EtOH alone caused a significant decrease in expression in the control group (H_2O) at all tested concentrations ($p < 0.05$), with the strongest reduction observed at 1.0% EtOH. Each of the tested withanolides also reduced *grin3a* expression in the EtOH-free groups.

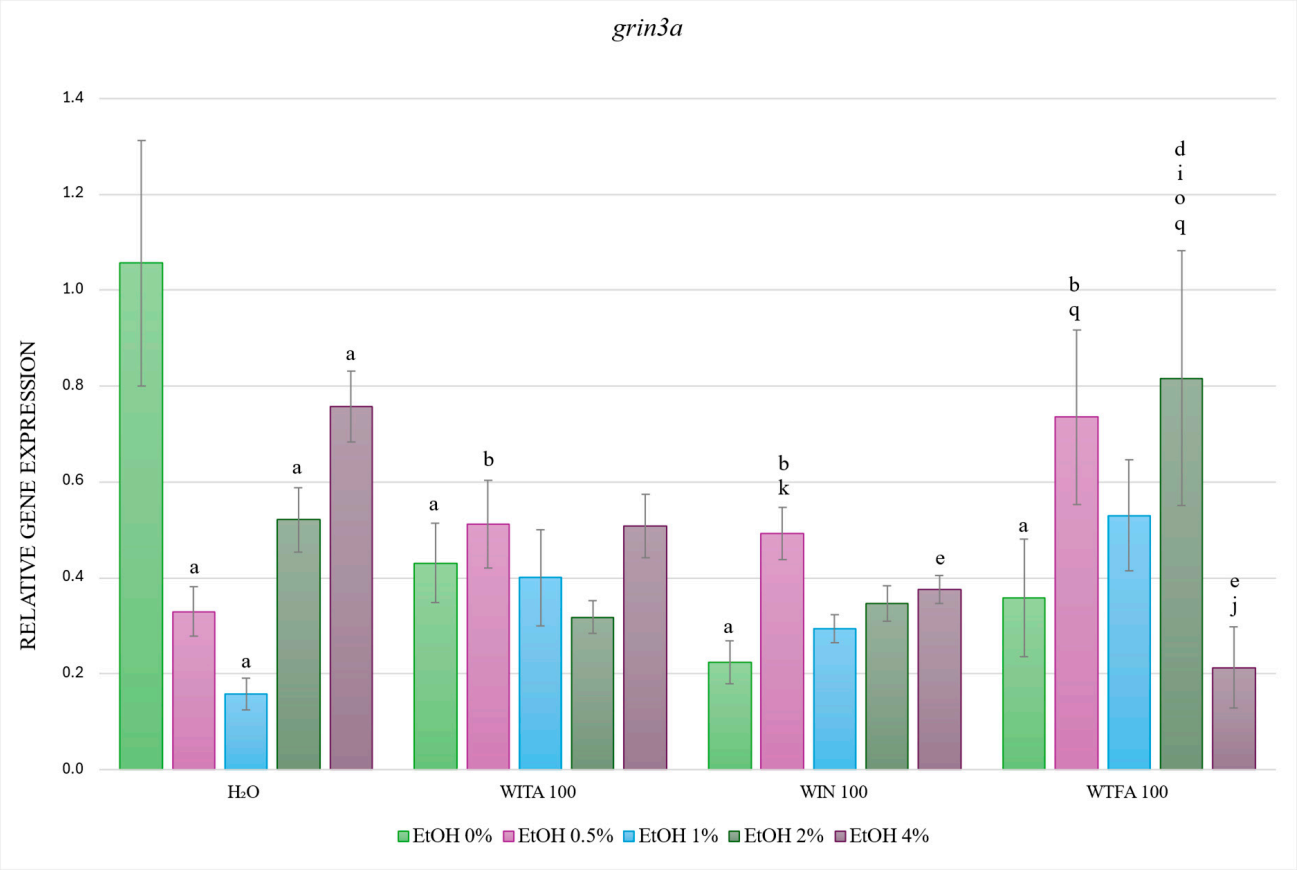


Figure 8. Effect of WITA, WIN and WTFA on *grin3a* mRNA expression in *D. rerio* larvae exposed to an EtOH gradient (0–4.0%). Significant comparisons ($p < 0.05$): a vs. H_2O; b vs. H_2O 0.5%; d vs. H_2O 2%; e vs. H_2O 4%; i vs. WITA 2%; j vs. WITA 4%; k vs. WIN 0%; o vs. WIN 2%; q vs. WTFA 0%. Data are presented as mean ± SEM.

Administration of WITA or WIN flattened the biphasic effect of EtOH. In the WITA group, no significant within-group differences between EtOH concentrations were observed, whereas in the WIN group minor differences were detected compared with the respective control conditions (0.5% and 4% EtOH, $p < 0.05$). The most pronounced effect was observed after the WTFA administration. In this case, WTFA in combination with EtOH increased *grin3a* expression relative to WTFA 0% (significantly at 0.5% and 2.0%, $p < 0.05$), as well as relative to the corresponding concentrations in the H_2O, WITA, and WIN groups (also at 0.5% and 2% EtOH, $p < 0.05$). At 4.0% EtOH, however, a decrease was observed compared with the group that did not receive any withanolide.

In the studies investigating the effects of an EtOH gradient and withanolides on *grin3ba* gene expression, statistically significant changes were observed for the EtOH effect [F (4134) = 26.144, $p < 0.001$] and for the withanolides [F (3134) = 188.59, $p < 0.001$], as

well as for their interaction [F (12,134) = 42.232, $p < 0.001$], as shown in Figure 9. Detailed post hoc analysis revealed that EtOH alone caused a significant decrease in expression in the control group (H_2O) at all EtOH concentrations ($p < 0.05$). Each of the withanolides also caused a significant decrease in *grin3ba* expression. In the WITA group, 0.5% EtOH caused a significant increase in expression, whereas in the WIN group, an overall flattening was observed. Once again, the greatest changes were observed in the WTFA group, where its co-administration with EtOH resulted in statistically significant increases in expression at each concentration, both compared to the WTFA control group and to groups receiving EtOH alone without withanolide, as well as to groups receiving WITA and WIN simultaneously with EtOH.

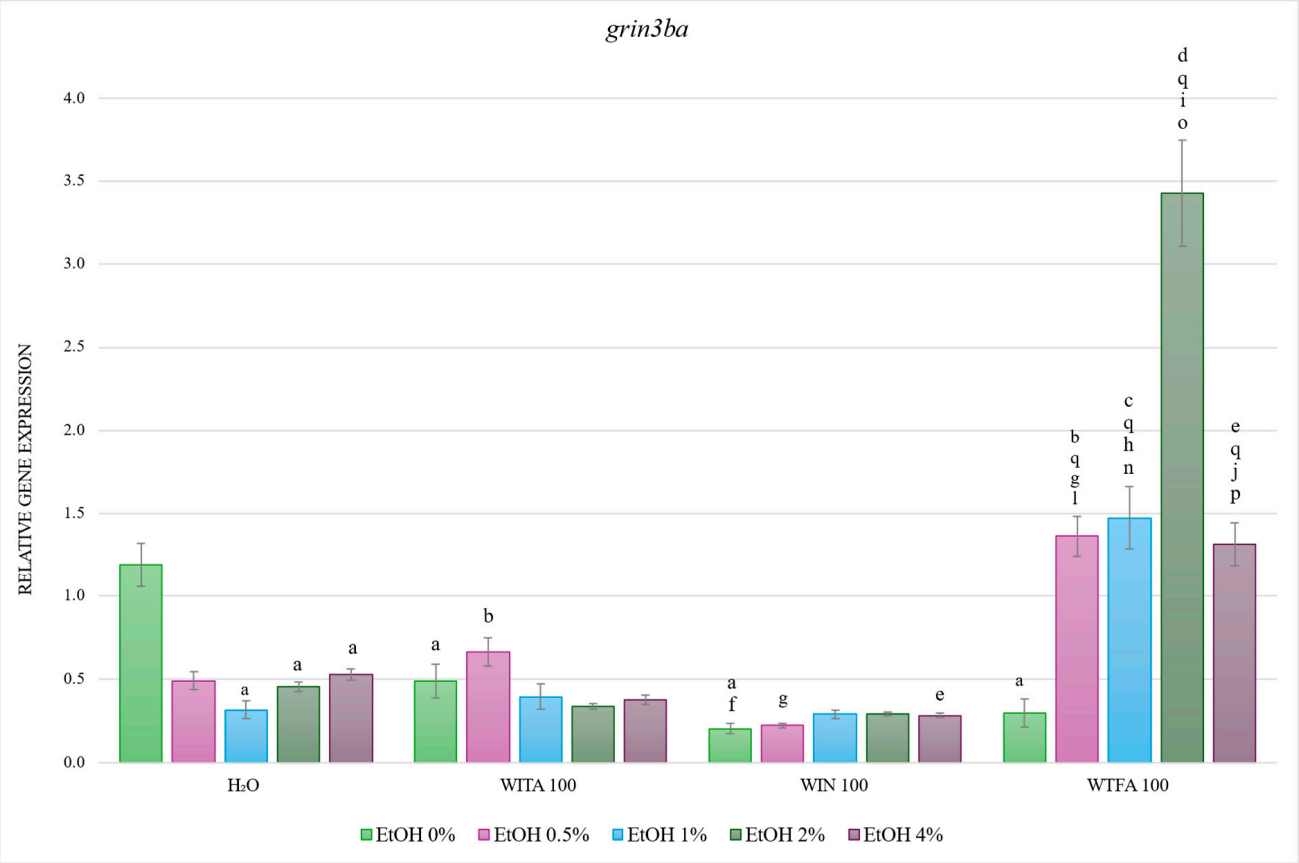


Figure 9. Effect of WITA, WIN and WTFA on *grin3ba* mRNA expression in *D. rerio* larvae exposed to an EtOH gradient (0–4.0%). Significant comparisons ($p < 0.05$): a vs. H_2O; b vs. H_2O 0.5%; c vs. H_2O 1%; d vs. H_2O 2%; e vs. H_2O 4%; f vs. WITA 0%; g vs. WITA 0.5%; h vs. WITA 1%; i vs. WITA 2%; j vs. WITA 4%; l vs. WIN 0.5%; n vs. WIN 1%; o vs. WIN 2%; p vs. WIN 4%; q vs. WTFA 0%. Data are presented as mean ± SEM.

4. Discussion

The present study was designed as a direct complement and extension to our previously published investigation of the GABAergic component of acute EtOH–withanolide interactions [15], extending the analysis to the glutamatergic system using the same experimental specimens, dosing, and behavioral protocol. We combined a behavioral readout, the DLCI parameter, with transcriptional profiling of four NMDA receptor subunit genes, allowing the photokinetic response and NMDA receptor subunit transcription to be examined in larvae from the same experimental groups. Because RNA was extracted from pools of eight larvae, whereas the DLCI was calculated for individual larvae, the two endpoints can be related only at the group level, as co-occurring responses to the same treatments, and not as

an individual-level association. At the transcriptional level, the four subunit genes revealed a consistent pattern that both complements and contrasts with the GABAergic findings: acute EtOH was associated with GluN2-type subunit upregulation alongside GluN3-type downregulation, and the three withanolides modulate this response in ways that differ markedly between compounds.

At the behavioral level, the DLCI evaluation revealed a clear concentration-dependent effect of acute EtOH. Photokinetic differentiation was preserved at 0.5% and 1.0% EtOH, where DLCI values were indistinguishable from the H_2O control. It then declined sharply at 2.0% and was effectively abolished at 4.0%, where values fell to around zero. A DLCI value close to zero indicates that locomotion is no longer linked to lighting conditions. The larvae moved at similar levels in light and dark and lost their normal preference for movement in the dark. This loss of differentiation at high EtOH is consistent with the sedative phase of EtOH biphasic action. It reflects a high-dose breakdown of sensory-motor coupling rather than a simple change in overall activity, which the normalized index is designed to discount.

This behavioral profile is mechanistically relevant because larval zebrafish locomotion is sensitive to NMDA-receptor antagonism by 5 dpf [26], and the light–dark locomotor response engages glutamatergic circuitry [25,53]. The DLCI therefore provides a behavioral readout that is plausibly coupled to the glutamatergic system probed at the transcriptional level, although a direct NMDA-receptor dependence of the photokinetic differentiation itself remains to be demonstrated pharmacologically. The concentrations at which photokinetic differentiation collapsed, namely 2.0% and 4.0% EtOH, coincide with those at which *grin2aa* transcription was most strongly upregulated, whereas *grin2bb* mRNA levels were already elevated across the gradient. One interpretation compatible with these data is that, at high EtOH concentrations, NMDA receptor function is inhibited sufficiently to disrupt the photokinetic response, and that the upregulation of GluN2-type subunit transcripts represents a compensatory response to this hypofunction [4,61]. However, neither receptor activity nor subunit protein abundance was measured here, so this mechanism is proposed rather than demonstrated. This correspondence is a group-level co-occurrence. The behavioral and transcriptional measures were obtained from the same experimental groups, but RNA was analyzed in pools of eight larvae, whereas the DLCI was determined for individual larvae; the present design therefore cannot establish an individual-level association between the two endpoints, nor that the transcriptional changes cause the behavioral changes.

The three withanolides modulated this EtOH effect to differing and comparatively modest degrees. This is consistent with the much smaller effect sizes for the withanolide factor than for the EtOH factor in all four analyses. WITA was the only compound that preserved photokinetic differentiation under high EtOH, and only at its highest concentration. At WITA 500, the DLCI remained positive at 4.0% EtOH, and no significant within-group decline was detected. This behavioral buffering is directionally consistent with the reported capacity of WITA to normalize NMDA receptor function under pathological conditions and with the attenuation of EtOH-induced transcriptional changes described below. The protective behavioral effect emerged at a concentration above the 100 µg/L used for transcriptional profiling, so the two datasets cannot be mapped dose for dose, and the convergence should be read as general rather than quantitative. WIN did not preserve differentiation. At its highest concentration, it deepened the DLCI reduction at 4.0% EtOH. This agrees with the limited response of NMDA receptor subunit transcripts to WIN and would be compatible with the hypothesis, which remains to be tested functionally, that WIN acts preferentially through GABAergic mechanisms [15]. WTFA likewise did not rescue the high-EtOH collapse: DLCI was reduced at 2.0% and 4.0% EtOH at every WTFA concentration, without a significant difference from the corresponding withanolide-free groups. This is compatible with the possibility that WTFA potentiates rather than offsets the depressant action of EtOH,

in line with its synergistic transcriptional response and with the potentiated locomotor suppression reported in our previous GABAergic study [15].

Transcription of *grin2aa* increased significantly at 2.0% and 4.0% EtOH, with the strongest upregulation at 4.0%. In contrast, *grin2bb* was upregulated at all tested EtOH concentrations (0.5–4.0%), indicating a lower threshold of sensitivity to acute EtOH. This difference in concentration sensitivity between the two co-orthologues is pharmacologically consistent with the established higher sensitivity of GluN2B-containing receptors to EtOH inhibition, attributed to both kinetic and structural differences at the subunit level [39,40]. If the upregulation reflects a compensatory response to receptor inhibition, stronger inhibition of GluN2B-containing receptors would be expected to produce a more sensitive transcriptional response, in line with our observation that *grin2bb* transcripts were already upregulated at 0.5% EtOH, a concentration at which *grin2aa* ones remain unchanged. This finding is consistent with the broader literature identifying GluN2B upregulation as the reproducible response to EtOH across experimental models [62].

It is worth noting that in adult mammalian systems, acute EtOH has been reported to increase GluN2A and GluN2B protein without corresponding mRNA changes [63]. That points to post-transcriptional regulation taking over in a mature context. In the present zebrafish larvae at 5 dpf, by contrast, all four genes showed pronounced transcriptional responses. One interpretation is that a still-maturing nervous system, in which the GluN2B-to-GluN2A transition is under way [18,27], is more transcriptionally plastic and therefore more sensitive to pharmacological perturbation. Abramova et al. [24] recently showed that the electrophysiological differences between receptors containing zebrafish GluN2Aa/Ab and GluN2Bb parallel those between mammalian GluN2A- and GluN2B-containing receptors, and that *grin2a* loss of function in zebrafish larvae increases locomotor activity and may shift the receptor population towards GluN2B; this supports both the translational relevance of the present model and the assumption that *grin2* paralogues retain subunit-specific pharmacology.

The GluN3-type subunits responded in the opposite direction. Both *grin3a* and *grin3ba* mRNAs levels decreased significantly at all tested EtOH concentrations, with the strongest reduction observed at 1.0% for *grin3a*. The functional significance of this downregulation is best understood in the context of GluN3A modulatory role. Unlike GluN2 subunits, which confer high conductance and Ca^{2+} permeability, incorporation of GluN3A dampens receptor activity, reducing single-channel conductance and Ca^{2+} influx and increasing Mg^{2+} sensitivity [20,21]. During development, this "brake" prevents premature synaptic stabilization [20,64,65]. If the reduced *grin3a* and *grin3ba* transcript levels translate into fewer GluN3-containing receptors, acute EtOH would be expected to release this brake, a mechanism operating in parallel with GluN2-type upregulation but through a distinct route. Both changes point in the same direction, towards greater NMDA-mediated excitatory capacity, which is consistent with a compensatory response to acute receptor inhibition. This interpretation remains inferential. The existing literature on GluN3A and EtOH is limited and comes from experimental contexts very different from ours. Jin et al. [47] reported elevated GluN3A mRNA in the hippocampus and orbitofrontal cortex of chronic alcoholics post-mortem, and Brady et al. [66] showed increased GluN3A protein after prenatal EtOH exposure in rodents-both representing prolonged exposure paradigms in mammalian systems. The opposite direction of change relative to our acute larval model does not necessarily indicate a contradiction, but rather may reflect distinct temporal phases of the adaptive response. In chronic paradigms, where sustained GluN2 upregulation has already occurred, GluN3A upregulation could instead serve to limit Ca^{2+} permeability of the overexpressed receptor population—a protective rather than compensatory adaptation. This possibility is consistent with the low sensitivity of GluN1/GluN3 receptors to EtOH

inhibition [43,67]. No study, however, has followed GluN3A regulation across the transition from acute to chronic exposure within a single model, and the proposed link therefore remains speculative.

The *grin3ba* findings are particularly noteworthy because, to our knowledge, no published data exist on GluN3B expression changes in response to EtOH. The available literature on GluN3B is limited to basic characterization of expression patterns [68], the behavioral phenotype of knockout mice showing impaired motor learning and cognition [69], and emerging evidence linking GluN3B to psychiatric disorders including schizophrenia and substance use disorders [70]. Our data provide novel evidence that both members of the GluN3 subfamily are transcriptionally responsive to acute EtOH. *grin3a* response—with maximal downregulation at 1.0% and partial recovery at higher concentrations—is difficult to explain with the available data. One speculative possibility is that it reflects the biphasic nature of EtOH's inhibition of NMDA receptors more broadly: Boikov et al. [71] described a high-affinity Ca^{2+}-dependent and a low-affinity Ca^{2+}-independent component of EtOH action on NMDA receptor channels, which could engage different transcriptional responses at different concentrations. However, this mechanism was characterized for GluN1/GluN2 receptors and its relevance to GluN3A transcriptional regulation is unknown. It should also be noted that the main ANOVA for *grin3a* did not reach significance for the EtOH factor, although post hoc pairwise comparisons did detect significant differences—suggesting that the overall *grin3a* response to EtOH showed a less consistent and non-monotonic response to EtOH than that of the other three genes.

Before considering the interactions with EtOH, it is important to examine the independent effects of each withanolide, since these define the transcriptional starting point from which the EtOH interaction proceeds. WITA alone increases both *grin2aa* and *grin2bb* expression while reducing the *grin3a* and *grin3ba* transcript levels. In other words, it mimics EtOH's gene expression pattern, though likely through very different mechanisms. WITA has documented synaptogenic and neuroprotective properties: Kuboyama et al. [72] showed that it induced regeneration of both axons and dendrites and restored synaptic structures in neurons damaged by amyloid-β, and Soman et al. [73] demonstrated that it normalized NMDA receptor density in epileptic rats while reversing memory deficits. Dar et al. [74] also showed WITA shields against glutamate-induced toxicity via MAPK blockade and PI3K/Akt activation. Thus, the increase in *grin2* subunit expression could reflect pro-synaptic, adaptive effects rather than compensation for inhibition. WIN produced the most modest baseline effects. For *grin2aa*, the only significant comparison was with the WITA group, while for *grin2bb*, changes were limited. WIN alone did, however, significantly reduce *grin3a* and *grin3ba* expression, consistent with the general pattern of GluN3-type downregulation observed across all three withanolides. This minimal transcriptional impact is consistent with WIN's proposed mechanism of action, which operates downstream of the receptor. Dar et al. [75] showed that WIN protects against NMDA-induced excitotoxicity by reducing Ca^{2+} accumulation, reactive oxygen species, and caspase activation—intracellular events that do not necessarily require changes in receptor subunit transcription. Such a mechanism need not alter receptor gene expression directly, which is consistent with the present transcriptional data. WTFA alone also shifted all four genes, although not markedly more than WITA or WIN; its distinctive profile emerged only in combination with EtOH, as discussed below. In silico work suggests that WS constituents can occupy allosteric sites on GluN2B-containing receptors: Kumar and Patnaik [76] docked WS phytochemicals against GluN2B, and Vashisth et al. [77] screened 80 WS constituents against the GluN1b/GluN2B complex, obtaining binding energies between −4.1 and −11.9 kcal/mol, with 17α-hydroxywithanolide D rather than WITA or WTFA emerging as the highest-ranking ligand. These are computational predictions only, and no experimental evidence of

direct binding of any withanolide to the NMDA receptor has been reported. If true, such an interaction might explain the pronounced effects observed when WTFA and EtOH are given together. Importantly, all three withanolides tend to lower baseline grin3a/ba, though likely by different mechanisms-a shift in NMDA composition worth probing further downstream.

These compound-specific patterns are consistent with those reported for the GABAergic system [15], where all three withanolides reduced *gabra1* and *gabra2* but diverged in their effects on *gabrd* and *gabrg2*. Both studies consistently show that each purified withanolide produces a different pattern of subunit expression changes at both GABAA and NMDA receptors.

The most informative results emerge from combining withanolides with EtOH, in which the three compounds produced fundamentally different outcomes. WITA modified the EtOH-induced transcriptional response in a gene-specific manner. For *grin2aa*, WITA elevated expression at baseline and at 0.5% EtOH relative to the corresponding H_2O groups, but no significant within-group differences were detected across EtOH concentrations within the WITA group—suggesting that WITA's effect on this subunit was not further augmented by increasing EtOH concentrations. For *grin2bb*, a different pattern was observed: EtOH within the WITA group progressively reduced expression relative to WITA alone, which is opposite to the upregulation seen in control larvae. For *grin3a* and *grin3ba*, WITA flattened the EtOH-induced biphasic response, eliminating the significant within-group variability observed in controls. This gene-specific modulation is consistent with reports that WITA can normalize NMDA receptor function under pathological conditions [72,73], and may involve direct receptor interaction—molecular docking studies have predicted that WITA binds allosterically to GluN2B-containing NMDA receptors [76,77]. If WITA does interact directly with NMDA receptors, the gene-specific pattern we observe may reflect the interplay between WITA's own receptor-level effects and the compensatory transcriptional response to EtOH-mediated inhibition, with the net outcome varying depending on subunit-specific regulatory dynamics. A similarly selective modulation was seen in our companion study, where WITA partly counteracted EtOH-induced changes in *gabra2* and *gabrg2* mRNA levels but not in gabra1 or *gabrd* [15], suggesting that, at the transcriptional level, the interaction of WITA with EtOH is subunit-selective rather than uniform.

From a translational perspective, WITA's capacity to attenuate EtOH-induced transcriptional changes is noteworthy. The compensatory upregulation of NMDA receptors that develops during EtOH exposure is a key contributor to withdrawal-associated hyperexcitability, seizures, and excitotoxic neuronal damage [4,62,78]. If WITA limits this upregulation, the receptor population upon cessation of EtOH exposure could theoretically be less prone to hyperexcitation. However, this interpretation is based on a larval zebrafish model under acute exposure conditions, and its relevance to mammalian systems or clinical scenarios remains to be established through chronic exposure paradigms in higher vertebrates.

WIN demonstrated the weakest interaction effects among the three compounds. Although isolated significant differences were detected for individual genes at specific EtOH concentrations, no consistent pattern of modulation emerged across the four subunits. This limited glutamatergic interaction contrasts with WIN's behavioral effects: in our companion study, WIN enhanced locomotion at low-to-moderate EtOH concentrations [15]. One possible explanation for this discrepancy is that the locomotor effects of WIN are mediated primarily through the GABAergic system, where WIN maintained broad suppression of GABAA receptor subunit transcription under EtOH—potentially weakening inhibitory neurotransmission and permitting greater motor output through disinhibition [79].

WTFA produced the largest and most consistent interaction effects across all four genes. For *grin2aa* and *grin2bb*, co-exposure with EtOH resulted in upregulation that far exceeded

the effects of either compound alone. For *grin3ba* transcripts, EtOH co-administration caused significant level increases at each concentration compared to WTFA alone, to EtOH-only controls, and to WITA and WIN groups. The *grin3a* mRNA-level response was more complex and similar to other withanolides: WTFA + EtOH increased expression at 0.5% and 2.0% relative to WTFA alone and to the other groups, but a decrease was observed at 4.0% EtOH. The pronounced *grin2*-type upregulation under combined WTFA + EtOH suggests a synergistic interaction at the transcriptional level. If both compounds inhibit NMDA receptor function—EtOH through established non-competitive inhibition [37,39,80] and WTFA through the predicted allosteric mechanism at GluN2B [76,77]—their combined inhibitory effect would produce a deeper reduction in Ca^{2+} influx through the channel. Since NMDA receptor expression is regulated by Ca^{2+} entering through the receptor channel, with reduced Ca^{2+} influx triggering compensatory upregulation of receptor subunits [61], a stronger combined inhibition would be expected to drive a proportionally stronger transcriptional response—which is consistent with the magnitude of *grin2aa* and *grin2bb* upregulation we observe. This explanation is, however, hypothetical: binding of WTFA to NMDA receptors has so far been predicted only in silico [76,77].

Interestingly, this massive GluN2 upregulation was accompanied by a reversal of *grin3*-type expression: while both WTFA alone and EtOH alone decreased *grin3a* and *grin3ba*, their combination at intermediate EtOH concentrations produced significant increases. This reversal may represent a secondary protective response—when the overexpression of high-conductance, Ca^{2+}-permeable GluN2-containing receptors reaches levels that could create excitotoxic risk, upregulation of GluN3 subunits would counterbalance this by limiting channel conductance and Ca^{2+} permeability upon incorporation into the receptor complex [16,20]. This molecular profile is consistent with WTFA behavioral effects in our companion study, where it potentiated locomotor suppression primarily at high EtOH concentrations while increasing GABAA subunit expression associated with stronger inhibitory signaling [15]. Taken together with the GABAergic findings, the current data are compatible with the hypothesis that WTFA enhances both components of EtOH's depressant action, i.e., GABAergic inhibition and NMDA receptor blockade. If confirmed functionally, such a dual enhancement would raise safety concerns. The degree of NMDA receptor subunit upregulation observed with combined WTFA + EtOH exposure substantially exceeds that with EtOH alone. Since compensatory NMDA receptor upregulation is a well-established mechanism contributing to withdrawal hyperexcitability and excitotoxic neuronal damage [81,82], the synergistic upregulation produced by WTFA co-administration could amplify this risk. Given the growing popularity of ashwagandha-based supplements [11] and the documented prevalence of concurrent EtOH use [12,13], this finding may be relevant for consumer safety.

Several methodological considerations are relevant. *D. rerio* larvae at 5 dpf are at an early developmental stage; although the zebrafish is an established model for translational neuroscience [83], receptor expression dynamics at this stage differ from those in adult zebrafish or mammals [35]. Larvae at the developmental stage used in this study are also at a point where GABAergic inhibition is still developing and may not be fully mature in all brain circuits at this age [28,30]. If some GABAergic signaling is still excitatory rather than inhibitory at this stage, it could make NMDA receptors easier to activate [16,32]. This may help explain why we observed strong mRNA changes here, while adult mammalian studies mostly report protein-level changes without matching mRNA changes [63]. The teleost-specific whole-genome duplication produces 13 NMDA receptor subunit genes, compared with 7 in mammals [33,35], and the extent of functional divergence between paralogues is not fully established. However, recent studies confirm structural and functional conservation between zebrafish and mammalian NMDA receptor orthologues [24,84].

Our analysis is limited to the transcriptional level. We are aware that the mRNA changes do not necessarily always translate into changes in protein expression, receptor assembly, membrane trafficking, or electrophysiological function. Discrepancies between NMDA receptor mRNA and protein expression have been documented after EtOH exposure [4,63,85]. Nonetheless, the internally consistent pattern across four subunit genes suggests biologically meaningful changes warranting investigation at the protein and functional levels.

Some design limitations should also be noted. Because RNA was isolated from pooled larvae, behavioral and transcriptional data can be related only at the group level. A minor contribution of DMSO cannot be fully excluded, although its concentrations were very low and identical across withanolides. Finally, larvae were treated as independent units, without modeling the experimental run as a separate factor.

We examined four of thirteen zebrafish NMDA receptor subunit genes. The obligatory GluN1 subunits (*grin1a*, *grin1b*) were not assessed, as their constitutive expression in all functional NMDA receptors makes them less informative for capturing subunit-specific pharmacological interactions. Other paralogues (e.g., *grin2ab*, *grin2ba*, *grin2ca*, *grin2cb*, *grin2da*, *grin2db*) were also not included and remain to be investigated. Furthermore, while all three withanolides are predicted to cross the blood–brain barrier [86] and have been detected in rat brain after oral administration [87], the pharmacokinetics of immersion delivery in zebrafish larvae remain insufficiently characterized [88,89]. Future studies should combine transcriptional analysis (including a spatial transcriptomics approach) with protein quantification and electrophysiological recordings, extend the investigation to adult zebrafish and mammalian models, and explore chronic exposure and withdrawal paradigms to test the safety predictions arising from the present data.

5. Conclusions

This study shows that acute EtOH disrupts photokinetic behavior in zebrafish larvae and reshapes the expression of NMDA receptor subunit genes, and that three structurally related withanolides modulate these effects in compound-specific manners. Acute EtOH produced a concentration-dependent loss of photokinetic differentiation: larvae still distinguished conditions at 0.5% and 1.0% EtOH, whereas at 2.0% and 4.0% the DLCI collapsed and locomotion no longer tracked changes in illumination. At the transcriptional level, EtOH upregulated *grin2aa* and *grin2bb* and downregulated *grin3a* and *grin3ba*. The *grin2bb* responded already at 0.5% EtOH, in line with the known higher EtOH sensitivity of GluN2B-containing receptors. The behavioral collapse coincided with the strongest *grin2aa* transcription induction; however, this association was observed at the group level only and was correlative. The three withanolides diverged clearly. WITA was the only compound that preserved photokinetic differentiation under high EtOH (at 500 µg/L), and it attenuated selected EtOH-induced transcriptional changes. WIN had minimal effects on both the DLCI and NMDA mRNA receptor subunit expression, suggesting that its central actions may depend mainly on other mechanisms. WTFA did not prevent the behavioral impairment but, combined with EtOH, drove *grin2*-type mRNA-level upregulation well beyond that seen with EtOH alone and, at intermediate EtOH concentrations, reversed the EtOH-induced decrease in *grin3*-type transcripts. The WTFA-EtOH interaction carries the clearest practical message, as it may raise safety concerns for consumers who combine WS preparations with EtOH. Because the study was performed in larvae, after acute exposure, and at the transcriptional level, these findings require validation at the protein and functional levels, in chronic paradigms and in the long term in mammalian models before they can be extrapolated to humans.

Author Contributions: Conceptualization, K.C.-P., M.S., R.K. and P.M.; methodology, K.C.-P., M.S., R.K. and E.C.; validation, K.C.-P., W.J., R.K. and E.C.; investigation, K.C.-P., W.J. and M.M.; formal analysis, K.C.-P. and M.S.; data curation, M.S. and P.M.; writing—original draft preparation, K.C.-P. and W.J.; writing—review and editing, M.S., R.K. and P.M.; visualization, K.C.-P.; supervision, P.M. All authors have read and agreed to the published version of the manuscript.

Funding: This research was funded by the statutory funds of the Department of Pharmacology, Poznan University of Medical Sciences, and by a grant awarded to the Student Scientific Society of Pharmacology in the STN Top Projekt competition (no. TOP0000011, 2025 edition).

Institutional Review Board Statement: Ethical approval was not required for this study, as experiments were performed on zebrafish larvae up to 5 days post-fertilization, which are not subject to animal experimentation legislation (Directive 2010/63/EU).

Informed Consent Statement: Not applicable.

Data Availability Statement: The data presented in this study are available on request from the corresponding author. The data are not publicly available due to the large volume of the raw experimental files (multiple EthoVision datasets totaling several terabytes), which makes public deposition technically and logistically impractical.

Acknowledgments: The authors would like to thank the Animal Facility, Poznan University of Medical Sciences, for providing and maintaining the zebrafish used in this study.

Conflicts of Interest: The authors declare no conflicts of interest.

Abbreviations

The following abbreviations are used in this manuscript:

ANOVA	Analysis of Variance
cDNA	complementary DNA
CNS	central nervous system
Ct	quantification cycle (threshold cycle)
DEPC	diethyl pyrocarbonate
DLCI	dark–light contrast index
DMSO	dimethyl sulfoxide
dpf	days post-fertilization
EtOH	ethanol
GABAA	γ-aminobutyric acid type A receptor
GluN	glutamate receptor, NMDA-type subunit (protein nomenclature)
mRNA	messenger ribonucleic acid
NMDA	N-methyl-D-aspartate
RNA	ribonucleic acid
RT	reverse transcription
RT-qPCR	real-time quantitative polymerase chain reaction with reverse transcription
SEM	standard error of the mean
WIN	withanone
WITA	withanolide A
WS	Withania somnifera
WTFA	withaferin A

References

1. World Health Organization. *Global Status Report on Alcohol and Health and Treatment of Substance Use Disorders*; World Health Organization: Geneva, Switzerland, 2024. Available online: https://www.who.int/publications/i/item/9789240096745 (accessed on 20 March 2026).
2. Manthey, J.; Kilian, C.; Carr, S.; Bartak, M.; Bloomfield, K.; Braddick, F.; Gual, A.; Neufeld, M.; O'Donnell, A.; Petruzelka, B.; et al. Use of alcohol, tobacco, cannabis, and other substances during the first wave of the SARS-CoV-2 pandemic in Europe: A survey on 36,000 European substance users. *Subst. Abuse Treat. Prev. Policy* **2021**, *16*, 36. [CrossRef] [PubMed]
3. Pohorecky, L.A. Biphasic action of ethanol. *Biobehav. Rev.* **1977**, *1*, 231–240. [CrossRef]

4. Chandrasekar, R. Alcohol and NMDA receptor: Current research and future direction. *Front. Mol. Neurosci.* **2013**, *6*, 14. [CrossRef] [PubMed]
5. Möykkynen, T.; Korpi, E.R. Acute effects of ethanol on glutamate receptors. *Basic Clin. Pharmacol. Toxicol.* **2012**, *111*, 4–13. [CrossRef] [PubMed]
6. Allgaier, C. Ethanol sensitivity of NMDA receptors. *Neurochem. Int.* **2002**, *41*, 377–382. [CrossRef] [PubMed]
7. Gilpin, N.W.; Koob, G.F. Neurobiology of alcohol dependence: Focus on motivational mechanisms. *Alcohol Res. Health* **2008**, *31*, 185–195. [PubMed]
8. Mikulska, P.; Malinowska, M.; Ignacyk, M.; Szustowski, P.; Nowak, J.; Pesta, K.; Szeląg, M.; Szklanny, D.; Judasz, E.; Kaczmarek, G.; et al. Ashwagandha (*Withania somnifera*)-Current Research on the Health-Promoting Activities: A Narrative Review. *Pharmaceutics* **2023**, *15*, 1057. [CrossRef] [PubMed]
9. Bashir, A.; Nabi, M.; Tabassum, N.; Afzal, S.; Ayoub, M. An updated review on phytochemistry and molecular targets of Withania somnifera (L.) Dunal (Ashwagandha). *Front. Pharmacol.* **2023**, *14*, 1049334. [CrossRef] [PubMed]
10. Grand View Research. Ashwagandha Supplements Market Size & Outlook. Available online: https://www.grandviewresearch.com/horizon/outlook/ashwagandha-supplements-market-size/global (accessed on 22 September 2026).
11. Zahiruddin, S.; Basist, P.; Parveen, A.; Parveen, R.; Khan, W.; Gaurav; Ahmad, S. Ashwagandha in brain disorders: A review of recent developments. *J. Ethnopharmacol.* **2020**, *257*, 112876. [CrossRef] [PubMed]
12. Lippert, A.; Renner, B. Herb-Drug Interaction in Inflammatory Diseases: Review of Phytomedicine and Herbal Supplements. *J. Clin. Med.* **2022**, *11*, 1567. [CrossRef] [PubMed]
13. Sivertsen, K.; Lukic, M.; Kristoffersen, A.E. Gender specific association between the use of complementary and alternative medicine (CAM) and alcohol consumption and injuries caused by drinking in the sixth Tromsø study. *BMC Complement. Altern. Med.* **2018**, *18*, 239. [CrossRef] [PubMed]
14. Candelario, M.; Cuellar, E.; Reyes-Ruiz, J.M.; Darabedian, N.; Feimeng, Z.; Miledi, R.; Russo-Neustadt, A.; Limon, A. Direct evidence for GABAergic activity of Withania somnifera on mammalian ionotropic GABAA and GABAρ receptors. *J. Ethnopharmacol.* **2015**, *171*, 264–272. [CrossRef] [PubMed]
15. Czora-Poczwardowska, K.; Kujawski, R.; Jarczak, W.; Cicha, E.; Mikołajczak, P.; Szulc, M. Ethanol-Withanolides Interactions: Compound-Specific Effects on Zebrafish Larvae Locomotor Behavior and GABAA Receptor Subunit Expression. *Int. J. Mol. Sci.* **2025**, *26*, 10991. [CrossRef] [PubMed]
16. Traynelis, S.F.; Wollmuth, L.P.; McBain, C.J.; Menniti, F.S.; Vance, K.M.; Ogden, K.K.; Hansen, K.B.; Yuan, H.; Myers, S.J.; Dingledine, R. Glutamate receptor ion channels: Structure, regulation, and function. *Pharmacol. Rev.* **2010**, *62*, 405–496. [CrossRef] [PubMed]
17. Hansen, K.B.; Yi, F.; Perszyk, R.E.; Furukawa, H.; Wollmuth, L.P.; Gibb, A.J.; Traynelis, S.F. Structure, function, and allosteric modulation of NMDA receptors. *J. Gen. Physiol.* **2018**, *150*, 1081–1105. [CrossRef] [PubMed]
18. Paoletti, P.; Bellone, C.; Zhou, Q. NMDA receptor subunit diversity: Impact on receptor properties, synaptic plasticity and disease. *Nat. Rev. Neurosci.* **2013**, *14*, 383–400. [CrossRef] [PubMed]
19. Cull-Candy, S.; Brickley, S.; Farrant, M. NMDA receptor subunits: Diversity, development and disease. *Curr. Opin. Neurobiol.* **2001**, *11*, 327–335. [CrossRef] [PubMed]
20. Pérez-Otaño, I.; Larsen, R.S.; Wesseling, J.F. Emerging roles of GluN3-containing NMDA receptors in the CNS. *Nat. Rev. Neurosci.* **2016**, *17*, 623–635. [CrossRef] [PubMed]
21. Crawley, O.; Conde-Dusman, M.J.; Pérez-Otaño, I. GluN3A NMDA receptor subunits: More enigmatic than ever? *J. Physiol.* **2022**, *600*, 261–276. [CrossRef] [PubMed]
22. González-González, I.M.; Gray, J.A.; Ferreira, J.; Conde-Dusman, M.J.; Bouchet, D.; Perez-Otaño, I.; Groc, L. GluN3A subunit tunes NMDA receptor synaptic trafficking and content during postnatal brain development. *Cell Rep.* **2023**, *42*, 112477. [CrossRef] [PubMed]
23. Saint-Amant, L.; Drapeau, P. Time course of the development of motor behaviors in the zebrafish embryo. *J. Neurobiol.* **1998**, *37*, 622–632. [CrossRef]
24. Abramova, V.; Tomovic, E.; Kysilov, B.; Korinek, M.; Dobrovolski, M.; Krausova, B.H.; Fili, K.; Abdel Rahman, F.E.S.; Bozikova, P.; Cerny, J.; et al. Disruption of *grin2A*, an Epilepsy-Associated Gene, Produces Altered Spontaneous Swim Behavior in Zebrafish. *J. Neurosci.* **2025**, *45*, e0946252025. [CrossRef] [PubMed]
25. Burgess, H.A.; Granato, M. Modulation of locomotor activity in larval zebrafish during light adaptation. *J. Exp. Biol.* **2007**, *210*, 2526–2539. [CrossRef] [PubMed]
26. Chen, J.; Patel, R.; Friedman, T.C.; Jones, K.S. The behavioral and pharmacological actions of NMDA receptor antagonism are conserved in zebrafish larvae. *Int. J. Comp. Psychol.* **2010**, *23*, 82–90. [CrossRef]
27. Chu, Y.; Xu, Y.; Huang, M.; Fang, X.; Huang, X.; Yao, Z.; Wu, J.; Zhou, N.; He, K.; Liu, Y.; et al. Linear ubiquitination of the NMDA receptor GluN2A subunit facilitates the GluN2B-to-GluN2A switch and synaptic maturation. *Proc. Natl. Acad. Sci. USA* **2026**, *123*, e2515389123. [CrossRef] [PubMed]

28. Reynolds, A.; Brustein, E.; Liao, M.; Mercado, A.; Babilonia, E.; Mount, D.B.; Drapeau, P. Neurogenic role of the depolarizing chloride gradient revealed by global overexpression of KCC2 from the onset of development. *J. Neurosci.* **2008**, *28*, 1588–1597. [CrossRef] [PubMed]
29. Zhang, R.; Wei, H.; Xia, Y.; Du, J. Development of light response and GABAergic excitation-to-inhibition switch in zebrafish retinal ganglion cells. *J. Physiol.* **2010**, *588*, 2557–2569. [CrossRef] [PubMed]
30. Rivera, C.; Voipio, J.; Payne, J.A.; Ruusuvuori, E.; Lahtinen, H.; Lamsa, K.; Pirvola, U.; Saarma, M.; Kaila, K. The K^+/Cl^- co-transporter KCC2 renders GABA hyperpolarizing during neuronal maturation. *Nature* **1999**, *397*, 251–255. [CrossRef] [PubMed]
31. Ben-Ari, Y.; Gaiarsa, J.-L.; Tyzio, R.; Khazipov, R. GABA: A pioneer transmitter that excites immature neurons and generates primitive oscillations. *Physiol. Rev.* **2007**, *87*, 1215–1284. [CrossRef] [PubMed]
32. Ben-Ari, Y. Excitatory actions of GABA during development: The nature of the nurture. *Nat. Rev. Neurosci.* **2002**, *3*, 728–739. [CrossRef] [PubMed]
33. Horzmann, K.A.; Freeman, J.L. Zebrafish get connected: Investigating neurotransmission targets and alterations in chemical toxicity. *Toxics* **2016**, *4*, 19. [CrossRef] [PubMed]
34. Meyer, A.; Schartl, M. Gene and genome duplications in vertebrates: The one-to-four (-to-eight in fish) rule and the evolution of novel gene functions. *Curr. Opin. Cell Biol.* **1999**, *11*, 699–704. [CrossRef] [PubMed]
35. Cox, J.A.; Kucenas, S.; Voigt, M.M. Molecular characterization and embryonic expression of the family of N-methyl-D-aspartate receptor subunit genes in the zebrafish. *Dev. Dyn.* **2005**, *234*, 756–766. [CrossRef] [PubMed]
36. Howe, K.; Clark, M.D.; Torroja, C.F.; Torrance, J.; Berthelot, C.; Muffato, M.; Collins, J.E.; Humphray, S.; McLaren, K.; Matthews, L.; et al. The zebrafish reference genome sequence and its relationship to the human genome. *Nature* **2013**, *496*, 498–503. [CrossRef] [PubMed]
37. Lovinger, D.M.; White, G.; Weight, F.F. Ethanol inhibits NMDA-activated ion current in hippocampal neurons. *Science* **1989**, *243*, 1721–1724. [CrossRef] [PubMed]
38. Wills, T.A.; Winder, D.G. Ethanol effects on N-methyl-D-aspartate receptors in the bed nucleus of the stria terminalis. *Cold Spring Harb. Perspect. Med.* **2013**, *3*, a012161. [CrossRef] [PubMed]
39. Peoples, R.W.; Ren, H. Effects of ethanol on GluN1/GluN2A and GluN1/GluN2B NMDA receptor-ion channel gating kinetics. *Alcohol. Clin. Exp. Res.* **2022**, *46*, 2203–2213. [CrossRef] [PubMed]
40. Zhao, Y.; Ren, H.; Dwyer, D.S.; Peoples, R.W. Different sites of alcohol action in the NMDA receptor GluN2A and GluN2B subunits. *Neuropharmacology* **2015**, *97*, 240–250. [CrossRef] [PubMed]
41. Otton, H.J.; Janssen, A.; O'Leary, T.; Chen, P.E.; Wyllie, D.J.A. Inhibition of rat recombinant GluN1/GluN2A and GluN1/GluN2B NMDA receptors by ethanol at concentrations based on the US/UK drink-drive limit. *Eur. J. Pharmacol.* **2009**, *614*, 14–21. [CrossRef] [PubMed]
42. Jin, C.; Smothers, C.T.; Woodward, J.J. Enhanced ethanol inhibition of recombinant N-methyl-D-aspartate receptors by magnesium: Role of NR3A subunits. *Alcohol Clin. Exp. Res.* **2008**, *32*, 1059–1066. [CrossRef] [PubMed]
43. Smothers, C.T.; Woodward, J.J. Effect of the NR3 subunit on ethanol inhibition of recombinant NMDA receptors. *Brain Res.* **2003**, *987*, 117–121. [CrossRef] [PubMed]
44. McClymont, D.W.; Harris, J.; Mellor, I.R. Open-channel blockade is less effective on GluN3B than GluN3A subunit-containing NMDA receptors. *Eur. J. Pharmacol.* **2012**, *686*, 22–31. [CrossRef] [PubMed]
45. Follesa, P.; Ticku, M.K. Chronic ethanol treatment differentially regulates NMDA receptor subunit mRNA expression in rat brain. *Brain Res. Mol. Brain Res.* **1995**, *29*, 99–106. [CrossRef] [PubMed]
46. Chandler, L.J.; Harris, R.A.; Crews, F.T. Ethanol tolerance and synaptic plasticity. *Trends Pharmacol. Sci.* **1998**, *19*, 491–495. [CrossRef] [PubMed]
47. Jin, Z.; Bhandage, A.K.; Bazov, I.; Kononenko, O.; Bakalkin, G.; Korpi, E.R.; Birnir, B. Selective increases of AMPA, NMDA, and kainate receptor subunit mRNAs in the hippocampus and orbitofrontal cortex but not in prefrontal cortex of human alcoholics. *Front. Cell. Neurosci.* **2014**, *8*, 11. [CrossRef] [PubMed]
48. Aleström, P.; D'Angelo, L.; Midtlyng, P.J.; Schorderet, D.F.; Schulte-Merker, S.; Sohm, F.; Warner, S. Zebrafish: Housing and husbandry recommendations. *Lab. Anim.* **2020**, *54*, 213–224. [CrossRef] [PubMed]
49. Westerfield, M. *The Zebrafish Book. A Guide for the Laboratory Use of Zebrafish (Danio rerio)*, 4th ed.; University of Oregon Press: Eugene, OR, USA, 2000.
50. Hallare, A.; Nagel, K.; Köhler, H.-R.; Triebskorn, R. Comparative embryotoxicity and proteotoxicity of three carrier solvents to zebrafish (*Danio rerio*) embryos. *Ecotoxicol. Environ. Saf.* **2006**, *63*, 378–388. [CrossRef] [PubMed]
51. Maes, J.; Verlooy, L.; Buenafe, O.E.; de Witte, P.A.M.; Esguerra, C.V.; Crawford, A.D. Evaluation of 14 Organic Solvents and Carriers for Screening Applications in Zebrafish Embryos and Larvae. *PLoS ONE* **2012**, *7*, e43850. [CrossRef] [PubMed]
52. Christou, M.; Kavaliauskis, A.; Ropstad, E.; Fraser, T.W.K. DMSO effects larval zebrafish (*Danio rerio*) behavior, with additive and interaction effects when combined with positive controls. *Sci. Total Environ.* **2020**, *709*, 134490. [CrossRef] [PubMed]

53. Li, F.; Lin, J.; Liu, X.; Li, W.; Ding, Y.; Zhang, Y.; Zhou, S.; Guo, N.; Li, Q. Characterization of the locomotor activities of zebrafish larvae under the influence of various neuroactive drugs. *Ann. Transl. Med.* **2018**, *6*, 173. [CrossRef] [PubMed]
54. Ennaceur, A.; Delacour, J. A new one-trial test for neurobiological studies of memory in rats. 1: Behavioral data. *Behav. Brain Res.* **1988**, *31*, 47–59. [CrossRef] [PubMed]
55. Akkerman, S.; Blokland, A.; Reneerkens, O.; van Goethem, N.P.; Bollen, E.; Gijselaers, H.J.M.; Lieben, C.K.J.; Steinbusch, H.W.M.; Prickaerts, J. Object recognition testing: Methodological considerations on exploration and discrimination measures. *Behav. Brain Res.* **2012**, *232*, 335–347. [CrossRef] [PubMed]
56. Chomczynski, P.; Sacchi, N. Single-step method of RNA isolation by acid guanidinium thiocyanate-phenol-chloroform extraction. *Anal. Biochem.* **1987**, *162*, 156–159. [CrossRef]
57. Houseright, R.A.; Rosowski, E.E.; Lam, P.-Y.; Tauzin, S.J.M.; Mulvaney, O.; Dewey, C.N.; Huttenlocher, A. Cell type specific gene expression profiling reveals a role for complement component C3 in neutrophil responses to tissue damage. *Sci. Rep.* **2020**, *10*, 15716. [CrossRef] [PubMed]
58. Livak, K.J.; Schmittgen, T.D. Analysis of relative gene expression data using real-time quantitative PCR and the 2(-Delta Delta C(T)) Method. *Methods* **2001**, *25*, 402–408. [CrossRef] [PubMed]
59. Bustin, S.A.; Wittwer, C.T. MIQE: A step toward more robust and reproducible quantitative PCR. *Clin. Chem.* **2017**, *63*, 1537–1538. [CrossRef] [PubMed]
60. Tang, R.; Dodd, A.; Lai, D.; McNabb, W.C.; Love, D.R. Validation of zebrafish (*Danio rerio*) reference genes for quantitative real-time RT-PCR normalization. *Acta Biochim. Biophys. Sin.* **2007**, *39*, 384–390. [CrossRef] [PubMed]
61. Chen, X.; Moore-Nichols, D.; Nguyen, H.; Michaelis, E.K. Calcium influx through NMDA receptors, chronic receptor inhibition by ethanol and 2-amino-5-phosponopentanoic acid, and receptor protein expression. *J. Neurochem.* **1999**, *72*, 1969–1980. [CrossRef] [PubMed]
62. Burnett, E.J.; Chandler, L.J.; Trantham-Davidson, H. Glutamatergic plasticity and alcohol dependence-induced alterations in reward, affect and cognition. *Prog. Neuropsychopharmacol. Biol. Psychiatry* **2016**, *65*, 309–320. [CrossRef] [PubMed]
63. Roh, M.-S.; Cui, F.J.; Kim, H.K.; Kang, U.G. Regulation of NMDA receptor subunits after acute ethanol treatment in rat brain. *Alcohol Alcohol.* **2011**, *46*, 672–679. [CrossRef] [PubMed]
64. Kehoe, L.A.; Bellone, C.; De Roo, M.; Zandueta, A.; Dey, P.N.; Pérez-Otaño, I.; Muller, D. GluN3A promotes dendritic spine pruning and destabilization during postnatal development. *J. Neurosci.* **2014**, *34*, 9213–9221. [CrossRef] [PubMed]
65. Chowdhury, D.; Marco, S.; Brooks, I.M.; Zandueta, A.; Rao, Y.; Haucke, V.; Wesseling, J.F.; Tavalin, S.J.; Pérez-Otaño, I. Tyrosine phosphorylation regulates the endocytosis and surface expression of GluN3A-containing NMDA receptors. *J. Neurosci.* **2013**, *33*, 4151–4164. [CrossRef] [PubMed]
66. Brady, M.L.; Diaz, M.R.; Iuso, A.; Everett, J.C.; Valenzuela, C.F.; Caldwell, K.K. Moderate prenatal alcohol exposure reduces plasticity and alters NMDA receptor subunit composition in the dentate gyrus. *J. Neurosci.* **2013**, *33*, 1062–1067. [CrossRef] [PubMed]
67. Smothers, C.T.; Woodward, J.J. Pharmacological characterization of glycine-activated currents in HEK 293 cells expressing N-methyl-D-aspartate NR1 and NR3 subunits. *J. Pharmacol. Exp. Ther.* **2007**, *322*, 739–748. [CrossRef] [PubMed]
68. Bendel, O.; Meijer, B.; Hurd, Y.; von Euler, G. Cloning and expression of the human NMDA receptor subunit NR3B in the adult human hippocampus. *Neurosci. Lett.* **2005**, *377*, 31–36. [CrossRef] [PubMed]
69. Niemann, S.; Kanki, H.; Fukui, Y.; Takao, K.; Fukaya, M.; Hynynen, M.N.; Churchill, M.J.; Shefner, J.M.; Bronson, R.T.; Brown, R.H.; et al. Genetic ablation of NMDA receptor subunit NR3B in mouse reveals motoneuronal and nonmotoneuronal phenotypes. *Eur. J. Neurosci.* **2007**, *26*, 1407–1420. [CrossRef] [PubMed]
70. Huang, Y.; Xie, J.; Chen, J.; Guo, S.; Li, Y.; Liu, F. Emerging roles of GluN3B NMDA receptor subunit in the central nervous system. *Neurosci. Bull.* **2026**, *42*, 663–678. [CrossRef] [PubMed]
71. Boikov, S.I.; Sibarov, D.A.; Antonov, S.M. Ethanol inhibition of NMDA receptors in calcium-dependent and -independent modes. *Biochem. Biophys. Res. Commun.* **2020**, *522*, 1046–1051. [CrossRef] [PubMed]
72. Kuboyama, T.; Tohda, C.; Komatsu, K. Neuritic regeneration and synaptic reconstruction induced by withanolide A. *Br. J. Pharmacol.* **2005**, *144*, 961–971. [CrossRef] [PubMed]
73. Soman, S.; Korah, P.K.; Jayanarayanan, S.; Mathew, J.; Paulose, C.S. Oxidative stress induced NMDA receptor alteration leads to spatial memory deficits in temporal lobe epilepsy: Ameliorative effects of Withania somnifera and Withanolide A. *Neurochem. Res.* **2012**, *37*, 1915–1927. [CrossRef] [PubMed]
74. Dar, N.J.; Satti, N.K.; Dutt, P.; Hamid, A.; Ahmad, M. Attenuation of Glutamate-Induced Excitotoxicity by Withanolide-A in Neuron-Like Cells: Role for PI3K/Akt/MAPK Signaling Pathway. *Mol. Neurobiol.* **2018**, *55*, 2725–2739. [CrossRef] [PubMed]
75. Dar, N.J.; Bhat, J.A.; Satti, N.K.; Sharma, P.R.; Hamid, A.; Ahmad, M. Withanone, an Active Constituent from Withania somnifera, Affords Protection Against NMDA-Induced Excitotoxicity in Neuron-Like Cells. *Mol. Neurobiol.* **2017**, *54*, 5061–5073. [CrossRef] [PubMed]

76. Kumar, G.; Patnaik, R. Exploring neuroprotective potential of Withania somnifera phytochemicals by inhibition of GluN2B-containing NMDA receptors: An in silico study. *Med. Hypotheses* **2016**, *92*, 35–43. [CrossRef] [PubMed]
77. Vashisth, M.K.; Hu, J.; Liu, M.; Basha, S.H.; Yu, C.; Huang, W. In-Silico discovery of 17alpha-hydroxywithanolide-D as potential neuroprotective allosteric modulator of NMDA receptor targeting Alzheimer's disease. *Sci. Rep.* **2024**, *14*, 27908. [CrossRef] [PubMed]
78. Quelch, D.; Lingford-Hughes, A.; John, B.; Nutt, D.; Bradberry, S.; Roderique-Davies, G. Promising strategies for the prevention of alcohol-related brain damage through optimised management of acute alcohol withdrawal: A focussed literature review. *J. Psychopharmacol.* **2025**, *39*, 652–666. [CrossRef] [PubMed]
79. Kumar, S.; Porcu, P.; Werner, D.F.; Matthews, D.B.; Diaz-Granados, J.L.; Helfand, R.S.; Morrow, A.L. The role of GABA(A) receptors in the acute and chronic effects of ethanol: A decade of progress. *Psychopharmacology* **2009**, *205*, 529–564. [CrossRef] [PubMed]
80. Wirkner, K.; Poelchen, W.; Köles, L.; Mühlberg, K.; Scheibler, P.; Allgaier, C.; Illes, P. Ethanol-induced inhibition of NMDA receptor channels. *Neurochem. Int.* **1999**, *35*, 153–162. [CrossRef] [PubMed]
81. Hoffman, P.L.; Tabakoff, B. The role of the NMDA receptor in ethanol withdrawal. *EXS* **1994**, *71*, 61–70. [CrossRef] [PubMed]
82. Lovinger, D.M. Excitotoxicity and alcohol-related brain damage. *Alcohol. Clin. Exp. Res.* **1993**, *17*, 19–27. [CrossRef] [PubMed]
83. Gerlai, R. Zebrafish antipredatory responses: A future for translational research? *Behav. Brain Res.* **2010**, *207*, 223–231. [CrossRef] [PubMed]
84. Nebet, E.R.; Aprea, C.; Zoodsma, J.D.; Raab, W.J.; Sirotkin, H.I.; Wollmuth, L.P. Conservation of human NMDA receptor subunits and disease variants in zebrafish. *BMC Genom.* **2025**, *26*, 1042. [CrossRef] [PubMed]
85. Acosta, G.; Hasenkamp, W.; Daunais, J.B.; Friedman, D.P.; Grant, K.A.; Hemby, S.E. Ethanol self-administration modulation of NMDA receptor subunit and related synaptic protein mRNA expression in prefrontal cortical fields in cynomolgus monkeys. *Brain Res.* **2010**, *1318*, 144–154. [CrossRef] [PubMed]
86. Modi, S.J.; Tiwari, A.; Ghule, C.; Pawar, S.; Saste, G.; Jagtap, S.; Singh, R.; Deshmukh, A.; Girme, A.; Hingorani, L. Pharmacokinetic Study of Withanosides and Withanolides from Withania somnifera Using Ultra-High Performance Liquid Chromatography-Tandem Mass Spectrometry (UHPLC-MS/MS). *Molecules* **2022**, *27*, 1476. [CrossRef] [PubMed]
87. Dadge, S.D.; Tiwari, N.; Husain, A.; Verma, S.; Agarwal, A.; Garg, R.; Rath, S.K.; Shanker, K.; Gayen, J.R. Simultaneous estimation of five biomarkers of neuroprotective herb Ashwagandha NMITLI-118R AF1 in rat plasma and brain using LC-ESI-MS/MS: Application to its pharmacokinetic and stability studies. *J. Chromatogr. B Analyt. Technol. Biomed. Life Sci.* **2023**, *1228*, 123834. [CrossRef] [PubMed]
88. Kantae, V.; Krekels, E.H.J.; Ordas, A.; González, O.; van Wijk, R.C.; Harms, A.C.; Racz, P.I.; van der Graaf, P.H.; Spaink, H.P.; Hankemeier, T. Pharmacokinetic Modeling of Paracetamol Uptake and Clearance in Zebrafish Larvae: Expanding the Allometric Scale in Vertebrates with Five Orders of Magnitude. *Zebrafish* **2016**, *13*, 504–510. [CrossRef] [PubMed]
89. van Wijk, R.C.; Krekels, E.H.J.; Kantae, V.; Harms, A.C.; Hankemeier, T.; van der Graaf, P.H.; Spaink, H.P. Impact of post-hatching maturation on the pharmacokinetics of paracetamol in zebrafish larvae. *Sci. Rep.* **2019**, *9*, 2149. [CrossRef] [PubMed]

Disclaimer/Publisher's Note: The statements, opinions and data contained in all publications are solely those of the individual author(s) and contributor(s) and not of MDPI and/or the editor(s). MDPI and/or the editor(s) disclaim responsibility for any injury to people or property resulting from any ideas, methods, instructions or products referred to in the content.